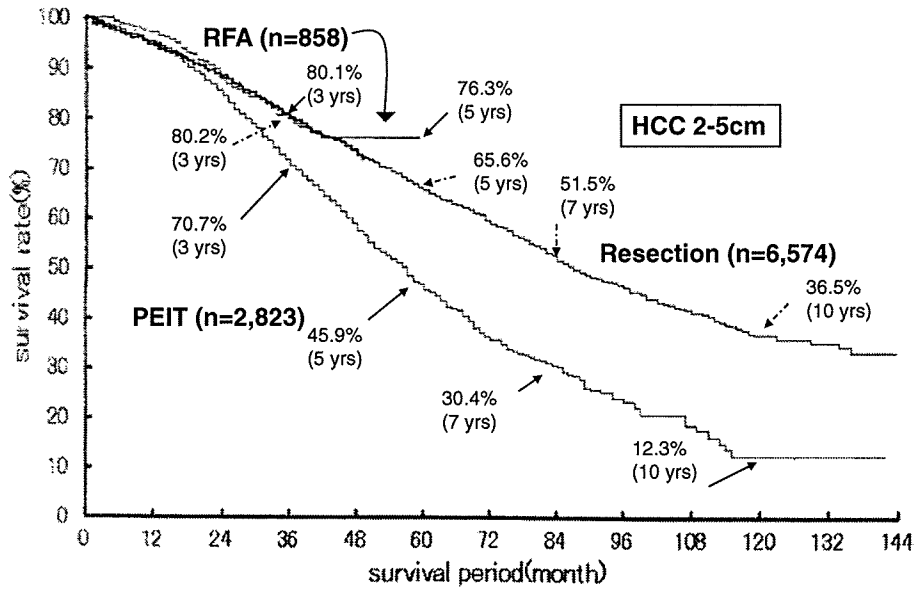

Fig. 6 Overall survival rate of single nodular HCCs of 2–5 cm in size with Child-Pugh A liver function treated by resection, percutaneous ethanol injection therapy (*PEIT*), radiofrequency ablation (*RFA*) according to the 17th nationwide survey by the Liver Cancer Study Group of Japan (LCSGJ)

Discussion

For resectable 2 to 5-cm tumors, surgery is the first choice because recurrence from a satellite lesion adjacent to the main lesion represents a poor-prognostic factor and it is more frequent after RFA. Regarding non-resectable liver cancer due to various reasons, such as a poor systemic condition, poor liver functional reserve, or in the elderly, favorable outcomes can be achieved by TACE followed by RFA in cases of 2 cm or larger hypervascular HCCs [6]. Certainly, it has to be pointed out that the disease-free survival rate was lower in our patients who were carriers of single 2 to 5-cm HCCs treated with RFA following TACE than the 5-year disease-free survival rate (31%) reported by Eguchi [7] and that in cases of anatomical resection (41%) reported by the Liver Cancer Study Group of Japan [5]. This is a further confirmation that surgery is the treatment of choice for resectable single HCCs 2–5 cm in size.

The overall disease-free survival rate of cases with single HCCs smaller than 5 cm, including both those lesions smaller than 2-cm or those ranging from 2 to 5 cm, treated by surgery has been reported to be lower than 40% by Poon et al. [8]. However, in the current study and those reported by the Liver Cancer Study Group of Japan after RFA substituted PEIT in the clinical practice, no significant differences were noticed in the overall survival between the surgery and RFA groups, suggesting that a favorable overall survival rate can be achieved in non-resectable Child-Pugh A cases with 2 to 5-cm HCCs by employing certain methods, such as RFA combined with preceding TACE. AFP, PIVKA-II, and the macroscopic gross type were extracted as prognosis-determining factors. Thus, the therapeutic strategy should be comprehensively determined based on these prognostic factors in addition to tumor size and liver function status.

In conclusion, single nodular HCC sized 2–5 cm in diameter can be successfully treated by a combination of RFA and proceeding TACE when operation is not indicated.

References

1. Bruix J, Sherman M, Practice Guidelines Committee, American Association for the Study of Liver Diseases. Management of hepatocellular carcinoma. Hepatology. 2005;42:1208–36.
2. Bruix J, Sherman M, Llovet JM, et al. Clinical management of hepatocellular carcinoma. Conclusions of the Barcelona-2000 EASL Conference. J Hepatol. 2001;35:421–30.
3. Makuuchi M. Development of evidence-based clinical guidelines for the diagnosis and treatment of hepatocellular carcinoma in Japan. Hepatol Res. 2008;38:37–51.
4. Kudo M, Okanoue T, Japan Society of Hepatology. Management of hepatocellular carcinoma in Japan: consensus-based clinical practice manual proposed by the Japan Society of Hepatology. Oncology. 2007;72:S2–15.
5. Ikai I, Arii S, Okazaki M, Okita K, Omata M, Kojiro M, et al. Report of the 17th Nationwide Follow-up Survey of Primary Liver Cancer in Japan. Hepatol Res. 2007;37:676–91.
6. Takahashi S, Kudo M, Chung H, Inoue T, Nagashima M, Kitai S, et al. Outcomes of nontransplant potentially curative therapy for early-stage hepatocellular carcinoma in Child-Pugh Stage A cirrhosis is comparable with liver transplantation. Dig Dis. 2007;25:303–9.
7. Eguchi S, Kanematsu T, Arii S, Okazaki K, Omata M, Ikai I, et al. Comparison of the outcomes between an anatomical subsegmentectomy and a non-anatomical minor hepatectomy for single hepatocellular carcinomas based on a Japanese nationwide survey. Surgery. 2008;143:469–75.
8. Poon RT. Liver transplantation for solitary hepatocellular carcinoma less than 3 cm in diameter in Child A cirrhosis. Dig Dis. 2007;25:334–40.

Eur Radiol (2009) 19 (Suppl 5): S975–S989
DOI 10.1007/s00330-009-1624-y

Consensus report of the 2nd International Forum for Liver MRI

Akihiro Tanimoto
Jeong Min Lee
Takamichi Murakami
Alexander Huppertz
Masatoshi Kudo
Luigi Grazioli

A. Tanimoto
Department of Diagnostic Radiology, Keio University School of Medicine, 35 Shinanomachi, Shinjuku-ku, Tokyo 160-8582, Japan

J.M. Lee
Department of Radiology, Seoul National University Hospital, 28 Yongon-dong, Chongno-gu, Seoul 110-744, Korea

T. Murakami
Department of Radiology, Kinki University School of Medicine, 377-2, Ohno-Higashi, Osaka-Sayama, Osaka 589-8511, Japan

A. Huppertz
Imaging Science Institute Charité, Berlin, Robert-Koch-Platz 7, 10115 Berlin, Germany

M. Kudo
Department of Gastroenterology and Hepatology, Kinki University School of Medicine,377-2 Ohno-Higashi, Osaka-Sayama, Osaka 589-8511, Japan

L. Grazioli (✉)
Department of Radiology, Civic Hospital of Brescia, University of Brescia, Piazzale Spedali Civili I, 25023 Brescia, Italy

Abstract Discussion at the 2nd Forum for Liver MRI: The International Primovist® User Meeting on the use of the hepatocyte-specific contrast agent gadolinium-ethoxybenzyl-diethylene triamine penta-acetic acid (Gd-EOB-DTPA) is reported. Changes to the currently recommended Gd-EOB-DTPA imaging protocol were identified that can reduce the overall examination time. The potential benefits of 3-T MR imaging using Gd-EOB-DTPA have yet to be fully explored. Data show that Gd-EOB-DTPA-enhanced MRI allows identification of liver lesions and provides a differential diagnosis of hepatocellular nodules in the non-cirrhotic and cirrhotic liver, based on vascularity, during the dynamic arterial, portal-venous and late phases, and during the hepatocyte-specific phase. Current European, American and Japanese guidelines for the diagnosis of hepatocellular carcinoma need to take into account the recent rapid advances in liver imaging. Based on published clinical trials and the experience of the attendees in the use of Gd-EOB-DTPA in liver imaging, a new simplified, non-invasive diagnostic algorithm was proposed that would be applicable to both Eastern and Western clinical practice in the evaluation of hepatocarcinogenesis and hepatocellular carcinoma. Preliminary clinical experience suggests that Gd-EOB-DTPA may also provide an innovative and cost-effective one-stop approach for staging rectal cancer using whole-body imaging.

Keywords Contrast-enhanced · Gadolinium-ethoxybenzyl-diethylene triamine pentaacetic acid · Gd-EOB-DTPA · Liver lesions · HCC · Magnetic resonance imaging · Metastases · Whole body

Introduction

Technical advances in magnetic resonance imaging (MRI) of the liver, in terms of hardware, software and contrast agents, have been made in recent years such that it now offers many advantages over computed tomography (CT) and ultrasonography (US) for liver imaging [1]. The non-specific extracellular contrast media for liver MRI include, among others, gadopentetate dimeglumine (Gd-DTPA, Magnevist®, Bayer Schering Pharma, Berlin, Germany), gadobutrol (Gadovist®, Bayer Schering Pharma, Berlin, Germany) and gadobenate dimeglumine (Gd-BOPTA, MultiHance®, Bracco Diagnostics Inc., Milan, Italy) [2]. Gadolinium-ethoxybenzyl-diethylene triamine penta-acetic acid (Gd-EOB-DTPA; Primovist®, Bayer Schering Pharma, Berlin, Germany; Eovist®, Bayer HealthCare Pharmaceuticals Inc.; EOB-Primovist, Bayer Schering Pharma, Osaka, Japan), also known as gadoxetic acid disodium, is a hepatocyte-specific contrast agent that is eliminated in equal quantities by the urinary and biliary systems [3, 4]. Gd-EOB-DTPA is specifically taken up by hepatocytes and thereby provides increased

lesion–liver contrast not achievable with the extracellular gadolinium-based contrast agents. Many features, including small injection volume, high relaxivity, low-level transient protein binding (10%) and the relatively low gadolinium dose (0.025 mmol/kg bw), distinguish the bolus-injected Gd-EOB-DTPA from the extracellular gadolinium-based contrast agents [5–7].

This document is derived from the discussion at the 2nd International Primovist® User Meeting, Kyoto, 17–18 October, 2008. Sixty-seven attendees, who came from Europe, Japan, Korea, Thailand and Australia, shared their individual experiences in the use of Gd-EOB-DTPA for liver imaging. In addition, they considered potential further uses of Gd-EOB-DTPA in MRI.

Optimization of the Gd-EOB-DTPA imaging protocol

Identification of hypervascular hepatocellular carcinomas (HCCs) involves arterial enhancement followed by washout in the portal-venous phase [8]. Gd-EOB-DTPA is used at a low dose; hence, the gadolinium content is one-quarter of the amount present in gadolinium-containing extracellular contrast media. This raises the question of whether or not the dynamic phase is similar and if adaptation of the protocol is needed.

The currently recommended protocol for Gd-EOB-DTPA-enhanced MRI comprises unenhanced in-/opposed-phase T1-weighted two-dimensional gradient-echo (with and without fat saturation), using a breath-hold technique, and two-dimensional T2-weighted fast spin-echo/turbo spin-echo (with fat saturation) sequences. A test bolus may then be administered, followed by a bolus injection of Gd-EOB-DTPA 0.1 ml/ kg body weight (dose 0.025 mmol/kg body weight) and T1-weighted three-dimensional gradient-echo (with fat saturation) imaging in breath-hold during the arterial (15–20 s post-injection), portal-venous (50–60 s) and 'equilibrium' (120 s) phases, and T1-weighted two-dimensional gradient-echo (with fat saturation and breath-hold) imaging in the hepatocyte-specific phase (20 min post-injection) [9]. This protocol is based on animal studies [10–13] and on clinical studies [4, 14–26]. The total examination time is approximately 30 min.

Timing of arterial-phase imaging

For contrast-enhanced CT, peak aortic enhancement based on physiological data and contrast-medium pharmacokinetics is the duration of infusion plus time of arrival of the contrast medium in the aorta and is dependent on cardiac output [27]. Maximal arterial-phase liver enhancement using CT occurs 6–8 s later [27]. However, peak aortic enhancement using gadolinium-enhanced MRI is more rapid and is the sum of aortic arrival time plus half the infusion time [28]. In contrast-enhanced MRI, the fixed-time method based on contrast-enhanced CT pharmacokinetics (30 s after contrast injection) using three-dimensional fast imaging with steady-state free precession (FISP), results in poorer arterial-phase visualization than the use of the test-injection method for the timing of the arterial-phase image [29]. Gd-EOB-DTPA is injected as bolus; the originally proposed injection speed was 2 ml/s. For optimal lesion enhancement it is no longer recommended anymore to use a fixed time to start the acquisition after injection because of individual factors affecting the arrival time of the bolus in the aorta and peak lesion enhancement. It is instead recommended to use a bolus timing technique. Although a test bolus can be used to calculate the aortic transit time, an automated bolus detection algorithm (MR SmartPrep; GE Medical Systems, Milwaukee, WI, USA; CARE Bolus, Siemens Medical Solutions, Erlangen, Germany) or fluoroscopic triggering (Bolus-Trak; Philips Medical Systems, Best, The Netherlands) is preferable [30–33].

For example, in the case of SmartPrep, the acquisition starts automatically after a signal threshold has been trespassed in the region of interest indicating the arrival of the bolus. A time delay can be set between arrival in aorta and start of acquisition in a way similar to contrast-enhanced CT imaging. However, unpublished data for Gd-EOB-DTPA suggest that one cannot extrapolate from CT data because the infusion duration is longer (2 ml/kg, 2 ml/s; i.e. 70 s for an average Western adult or 50 s for an average Japanese adult) for contrast-enhanced CT [27]. Preliminary data from a study in Japanese patients show that optimal enhancement in hypervascular HCC lesions using Gd-EOB-DTPA is achieved if the arterial-phase image is obtained 10–12 s after peak aortic enhancement (A. Tanimoto, personal communication).

The use of automatic triggering results in improved arterial-to-venous contrast and overcomes the need to take into account the patient's body weight, age, heart rate and cardiac output if using the fixed-time method.

Ringing artefacts are sometimes seen with contrast-enhanced MRI, but it is difficult to distinguish between such artefacts and image distortion due to patient movement, respiratory motion or other physiological processes. A small variation in bolus timing yields large variations in the appearance of the image, especially if the centre of k space was sampled in the vicinity of rapid variations in contrast medium concentration [34], and such artefacts occur most frequently if the centre of k space is acquired before the intravascular gadolinium concentration is maximal [35].

Consensus statement For optimal arterial-phase Gd-EOB-DTPA-enhanced MRI, automated bolus injection is recommended to avoid inconsistencies associated with manual timing and to minimize ringing artefacts.

Infusion rate of Gd-EOB-DTPA

Gd-EOB-DTPA is supplied in a prefilled 10-ml syringe. This volume should be sufficient for an adult of average body weight because the recommended dose is 0.1 ml/kg body weight. Administration can be performed manually, but an automatic injector is preferable. A Gd-EOB-DTPA injection rate of approximately 2 ml/s was originally proposed, based on the rate typically used for Gd-DTPA with FISP [36]. This infusion rate of 2 ml/s has been used extensively in clinical trials [14, 16, 19, 20, 24]. However, Zech (personal communication) has proposed that an infusion rate of 1 ml/s may be more appropriate [9], but may depend on the nature of the liver lesion. Data derived from a pig model suggest that Gd-EOB-DTPA injection at a rate of 1 ml/s is more effective [37]. Attendees reported little difference in the arterial-phase images obtained using 1 and 2 ml/s injection rates. Ringing artefacts observed during the arterial phase are dependent on duration of injection and seem to be less apparent with a slower injection rate and are less than with contrast-enhanced CT [35]. However, faster Gd-EOB-DTPA injection rates should be avoided as they could theoretically result in discomfort for the patient and pain at the injection site.

Consensus statement An infusion rate of 1–2 ml/s is recommended for Gd-EOB-DTPA-enhanced MRI.

Use of saline flush

A saline flush shortens the time until the contrast medium first appears in the hepatic artery [38]. For contrast-enhanced CT, a saline flush improves image quality and reduces artefacts [39, 40], with the volume of the saline chaser being based on body weight [41]. In the case of Gd-EOB-DTPA-enhanced MRI, the currently recommended saline flush volume is 20 ml, which should be administered at the same rate as the contrast medium. In some studies, a 30-ml saline flush was used [16, 19]. Employing two interconnected power injectors assists in delivering the saline chaser. However, backflow of contrast medium into the saline solution can occur, with the mixing of the contrast medium with saline solution resulting in dilution of the contrast medium. This can be avoided by the use of valves.

Consensus statement A saline chaser of 20–30 ml administered at the same rate as Gd-EOB-DTPA (1–2 ml/s) should be employed.

Reducing the examination time with Gd-EOB-DTPA

Optimal characterization of liver lesions requires imaging in the arterial, portal-venous and the so-called equilibrium phases in addition to unenhanced images [42] and, in the case of Gd-EOB-DTPA, during the hepatocyte-specific phase. Total imaging time may be reduced if the T2-weighted sequence is performed after, rather than before, contrast medium injection. If performed before Gd-EOB-DTPA administration, the total time for unenhanced T1-weighted and T2-weighted imaging is 10 min. By carrying out the T2-weighted imaging after the contrast medium injection, a saving of 5 min is possible.

Arterial and portal-venous vessels can be visualized (arterial and portal-venous phases, respectively) followed by an equilibrium phase 1–3 min after Gd-EOB-DTPA injection. The term "equilibrium phase" was originally applied to the last component of the dynamic liver MRI when using gadolinium-based extracellular contrast agents. For Gd-EOB-DTPA-enhanced imaging, it is not a true description because of the subsequent uptake of Gd-EOB-DTPA by the hepatocytes. The term "dynamic late phase", therefore, is considered more appropriate. For patients with normal liver function, late-phase imaging after 2 min is probably most effective. However, liver dysfunction may delay the wash-out of Gd-EOB-DTPA [43]; thus, for patients with cirrhosis, imaging at 3 min post-injection may be preferable.

Another factor that dictates the total imaging time is when the uptake of Gd-EOB-DTPA by the hepatocytes occurs. Until now, it has been assumed that maximal enhancement using Gd-EOB-DTPA is achieved after 20 min; this compares very favourably with the 40–120 min reported using Gd-BOPTA [44]. However, it may be possible to shorten the time from 20 min for the hepatocyte-specific phase imaging to 10 min and still observe Gd-EOB-DTPA uptake of sufficient quality for accurate diagnosis (L. Grazioli, personal communication). The decision to shorten the time should be based on prior clinic information; imaging after 20 min or later may be required for cirrhotic patients [45].

Consensus statement Performing T2-weighted imaging after Gd-EOB-DTPA injection helps to reduce total examination time. In addition, in non-cirrhotic patients, hepatocyte-phase imaging can be performed already at 10 min post-injection, thus shortening the overall examination time to 25 min.

Effect of serum bilirubin

Very high serum bilirubin concentrations can be associated with reduced Gd-EOB-DTPA enhancement. When serum bilirubin exceeds 51.3 μmol/l (3 mg/dl), despite reduced Gd-EOB-DTPA enhancement, signal intensity is still sufficient to be diagnostically effective (Bayer Schering Pharma, data on file). Signal intensities after 15 and 20 min are not significantly different when serum bilirubin levels are > 22.23 μmol/l (> 1.2 mg/dl)

(A. Tanimoto, personal communication) and impaired visualization of the biliary tree may occur, starting with total serum bilirubin levels of ≥30 μmol/l (≥1.75 mg/dl).

Consensus statement In patients with highly elevated serum bilirubin levels, despite reduced visualization of the biliary tree, performing hepatocyte-specific phase imaging 20 min after Gd-EOB-DTPA provides sufficient enhancement and diagnostically useful information for evaluation of focal liver lesions.

New protocol for Gd-EOB-DTPA-enhanced liver MRI

Using the currently recommended protocol, the total imaging time is between 30 and 35 min [9]. A revised protocol for Gd-EOB-DTPA-enhanced liver MRI using fast three-dimensional spoiled gradient echo sequences such as LAVA™ (Liver Acquisition with Volume Acceleration, GE Healthcare, Milwaukee, WI, USA), THRIVE™ (T1 High Resolution Isotropic Volume Expansion; Philips Medical Systems, Best, The Netherlands) and VIBE™ (Volumetric Interpolated Breath-hold Examination; Siemens Medical Solutions, Erlangen, Germany) results in a 10-min reduction in the total examination time (Table 1). The T1-weighted gradient-echo in-phase and opposed-phase (IP/OP) sequence is performed before the bolus injection of Gd-EOB-DTPA [46]. Improvements in breath-hold T1-weighted fast spoiled gradient-echo (used for IP/OP) and rapid T2-weighted single-shot echo-train acquisition (acronyms: SSFSE GEH; SShTSE Philips; HASTE Siemens) enable imaging with high spatial resolution in a single breath-hold [47]. This combination of sequences allows acquisition of the critical diagnostic information about both inherent T2-weighted and T1-weighted lesion contrast and lesion vascularity [48].

Discordance between spatial resolution of T1- and T2-weighted images

Although high-resolution T1-weighted images are achievable using Gd-EOB-DTPA and three-dimensional gradient-echo sequences enabling very small lesions to be visualized, the typical two-dimensional T2-weighted sequences do not provide comparable resolution.

3-T liver MRI

3-T MRI machines may increase the signal and the signal-to-noise ratio, thus yielding high-quality, thin-section T1-weighted three-dimensional gradient-echo images, but artefacts may be increased [49]. Direct comparisons of 3-T and 1.5-T liver imaging are infrequent. Signal-to-noise ratios for liver were significantly higher at 3.0 T using T2-weighted HASTE (half-Fourier acquisition single-shot turbo spin-echo) and a T1-weighted gradient-echo in- and opposed-phase sequence [50]. Using superparamagnetic iron oxide (SPIO)-enhanced MRI, stronger signal attenuation does not occur with 3-T versus 1.5-T [51]. One study suggests that the image quality of the 1.5-T non-contrast T1- and T2-weighted sequences is significantly better than with 3-T imaging [52].

Most attendees were satisfied with the Gd-EOB-DTPA-enhanced image quality using 1.5-T machines. Among the minority with access to 3-T machines, their use was generally restricted to research. Those with no experience of 3-T MRI had concerns that the pulse sequences used for 1.5-T liver MRI would not be applicable to 3-T.

There is currently no evidence whether two-dimensional fast low-angle shot (FLASH) or a three-dimensional gradient-echo sequence (e.g. VIBE™) is most appropriate for arterial-phase imaging; the latter may cause ringing artefacts. Attendees would welcome further research.

Consensus statement Although the 3-T MRI using Gd-EOB-DTPA has the potential for superior imaging, a greater likelihood of imaging artefacts was a concern. Data are required on whether two-dimensional FLASH or three-dimensional gradient-echo sequences (e.g. VIBE™) should be used for the arterial phase.

Table 1 Proposed new protocol for Gd-EOB-DTPA-enhanced liver MRI

- In-phase and opposed-phase fast spoiled gradient-echo sequence (SPGR GE Healthcare; T1-FFE Philips; FLASH 2D, Siemens)
- Pre-Gd-EOB-DTPA fast three-dimensional gradient-echo sequence (e.g. LAVA™, THRIVE™, VIBE™) (zip = 2, 1.5T), optional
- Gd-EOB-DTPA infusion (1–2 ml/s)
- Saline chaser (20–30 ml, 1–2 ml/s)
- Fast three-dimensional gradient-echo sequence in dynamic arterial phase (bolus timing)
- Fast three-dimensional gradient-echo sequence in dynamic portal-venous phase (70 s after Gd-EOB-DTPA administration)
- Fast three-dimensional gradient-echo sequence in dynamic late phase (2–3 min after Gd-EOB-DTPA administration)
- Heavy T2 single-shot fast-spin echo / T2-weighted fast-spin echo
- Diffusion-weighted imaging, optional
- Fast three-dimensional gradient-echo sequence in hepatobiliary phase – axial (10 min and/or 15 min and/or 20 min after Gd-EOB-DTPA administration)
- Fast three-dimensional gradient-echo sequence in hepatobiliary phase – sagittal and coronal (10 min after Gd-EOB-DTPA administration), optional

Characterization of lesions in non-cirrhotic liver

Comparison of dynamic vascular and parenchymal hepatocyte-specific Gd-EOB-DTPA-enhanced images enables detection of < 1-cm lesions and differentiation

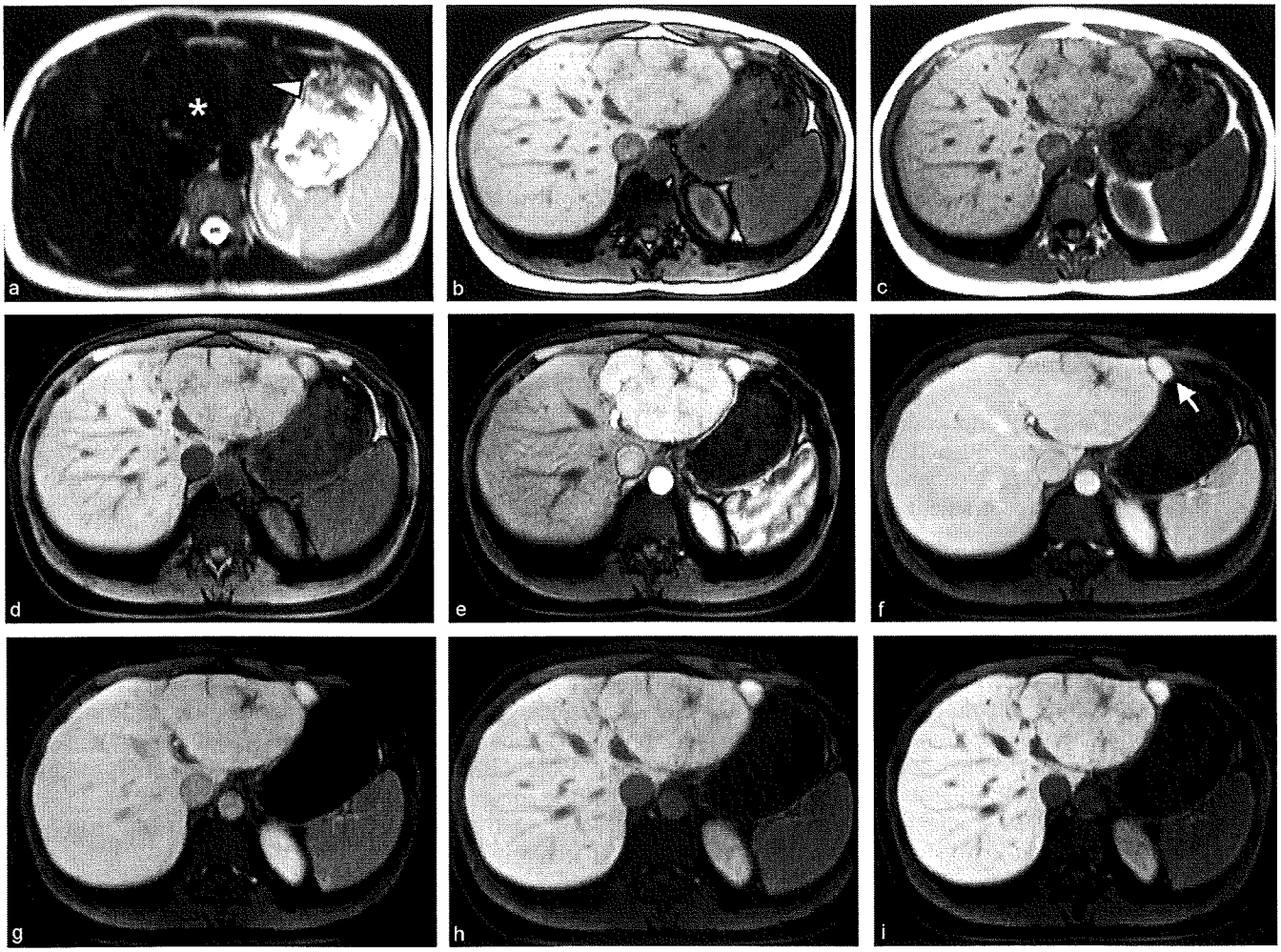

Fig. 1 Appearance of typical FNH with scar using Gd-EOB-DTPA-enhanced MRI (0.025 mmol/kg body weight). Precontrast: **a** T2-weighted image, large isointense, homogeneous, partially exophitic, solid lesion at II-III segment *(asterisk)* and eccentric hyperintense scar *(arrowhead)*. **b** T1-weighted out-phase. **c** In-phase and **d** GRE 3D T1 (VIBE) images with FNH nodule appearing isointense–slightly hypointense. Dynamic contrast-enhanced images. **e** Arterial phase with FNH nodule appearing hyperintense with homogeneous enhancement except for scar. **f** Portal-venous phase and **g** dynamic late phase FNH becoming iso-intense. Hepatobiliary phase images: **h** 10 and **i** 20 min after Gd-EOB-DTPA bolus injection FNH showing the same signal intensity compared with the surrounding parenchyma. Adjacent to the largest nodule, an additional small FNH nodule *(arrow)* shows similar signal intensity on unenhanced MRI, the same enhancement during the dynamic evaluation but appearing hyperintense in the hepatobiliary phase

between malignant and benign lesions with superior accuracy compared with helical CT [14, 15, 53].

Identification of hepatic haemangiomas

During the arterial phase, hepatic haemangiomas show peripheral globular enhancement and gradual fill-in through the portal-venous phase. Small haemangiomas may show rapid homogenous enhancement even in the arterial phase. However, because of the absence of hepatocytes, the lesion appears hypo-intense during the hepatocyte-specific phase using Gd-EOB-DTPA. Hepatic haemangiomas are easily identified by comparing the T1-weighted enhanced and T2-weighted unenhanced images.

Concensus statement Plain MRI, typical dynamic enhancement and T2-weighted images provide an important clue as to the presence of a hepatic haemangioma; hepatocyte-specific phase Gd-EOB-DTPA-enhanced MRI confirms the diagnosis.

FNHs and adenomas

Solid-type focal nodular hyperplasias (FNHs) display hepatocyte proliferation but lack a central vein or portal tract, scar tissue often being present [54]. Biliary drainage is abnormal. Hepatocellular adenomas contain enlarged hepatocytes rich in fat and glycogen and lack a portal tract or biliary ducts. Telangiectatic FNHs share many morphological features with hepatic adenomas, including sinusoidal dilatation spaces and, consequently, it has been proposed that they should be more accurately termed "telangiectatic hepatic adenomas" [55].

Identification of classic FNHs

Unenhanced T1-weighted images of FNH typically appear iso- or hypo-intense and T2-weighted images are usually iso- or slightly hyperintense, often with a hyperintense central scar [56]. FNH visualization using Gd-EOB-DTPA-enhanced MRI is superior to unenhanced MRI alone or biphasic-enhanced spiral CT [57].

Following Gd-EOB-DPTA injection, FNHs appear hyperintense during the arterial phase using a T1-weighted sequence with fat saturation (Fig. 1). In the hepatocyte-specific phase lesions appear iso- or even hyperintense [57]. Another frequent feature of the hepatocyte-specific image is a central scar, which because of the absence of hepatocytes, appears hypointense. These observations correlated with the abnormal biliary duct system, which does not communicate with the surrounding biliary tree.

Gb-EOB-DTPA-enhanced MRI demonstrates the classic FNH vascularization, with wash-out detectable on the dynamic-late-phase image as also seen using extracellular gadolinium-containing contrast media. Iso- to hyperintensity in the hepatobiliary phase after Gd-EOB-DTPA injection allows differentiation between FNHs and hepatic adenomas.

Identification of hepatic adenomas using Gd-EOB-DTPA

Hepatic adenomas are enhanced only during the arterial phase, usually appearing hypo-intense in the centre of the lesion during the hepatobiliary phase (Fig. 2). This reflects the lack of biliary duct and portal tract. With Gd-EOB-DTPA, hypo-intensity can be seen 20 min post-injection [58]. Similarly, in the case of Gd-BOPTA, this is observable only at a later time point (40–120 min post-injection) [59]. Using mangafodipir, both FNHs and hepatic adenomas display similar hepatobiliary-phase enhancement after 60 min [60].

Consensus statement Gd-EOB-DTPA facilitates the differentiation between FNHs and hepatic adenomas using images obtained during the hepatobiliary phase, as FNH are iso- to hyperintense due to abnormal biliary drainage.

Characterization of hepatocellular nodules in the cirrhotic liver

Staging of carcinogenesis

The Liver Cancer Study Group of Japan (2007) has identified eight levels of hepatocellular nodular changes, ranging from large regenerative nodules to undifferentiated hepatocellular carcinoma (Table 2). The continuity of these histological changes and internal heterogeneity, however, makes hepatocarcinogenesis staging difficult using the histopathology of biopsy specimens. The gradual decrease in the intraportal blood flow is indicative of increasing malignancy [61, 62]. Signal intensity on unenhanced T1-weighted echo-spin MRI (dysplastic nodules hyperintense) and on T2-weighted echo-spin MRI (dysplastic nodules hypo-intense; HCC hyperintense) further assists in characterization [63]. Reticulo-endothelial function determined using SPIO-enhanced MRI distinguishes between the Kupffer-cell content of the lesion [64–66].

Gd-EOB-DTPA allows superior detection of small lesions compared with contrast-enhanced helical CT [14, 19, 26], but it is difficult to distinguish between dysplastic nodules and early HCC; dysplastic nodules appear iso-intense to the liver parenchyma due to blood supply from the portal vein [67, 68]. Nevertheless, high-grade dysplastic nodules can be regarded as borderline malignancy. Their presence warrants increased surveillance and is routine practice in Japan [69]. There is, however, some discrepancy between the Eastern and Western definitions of high-grade dysplastic nodules [70].

Consensus statement Gd-EOB-DTPA allows the detection of early pathological changes, thus extending the options for the management of cirrhotic patients. Further data on use of Gd-EOB-DTPA in grading cirrhotic lesions, as well as studies correlating MRI and pathological findings, are required.

Identification of HCC using Gd-EOB-DTPA

Data suggest that the mean sensitivity of Gd-EOB-DTPA-enhanced MRI is significantly superior to 64-slice CT for the detection of HCC [71]. The wash-in and wash-out observed with Gd-EOB-DTPA are highly reproducible and provide superior images to multidetector CT, as has been observed by most attendees. Typically, HCC appears hypo-intense using unenhanced T1-weighted MRI, but occasionally nodules appear hyperintense. This problem can be overcome by applying a subtraction

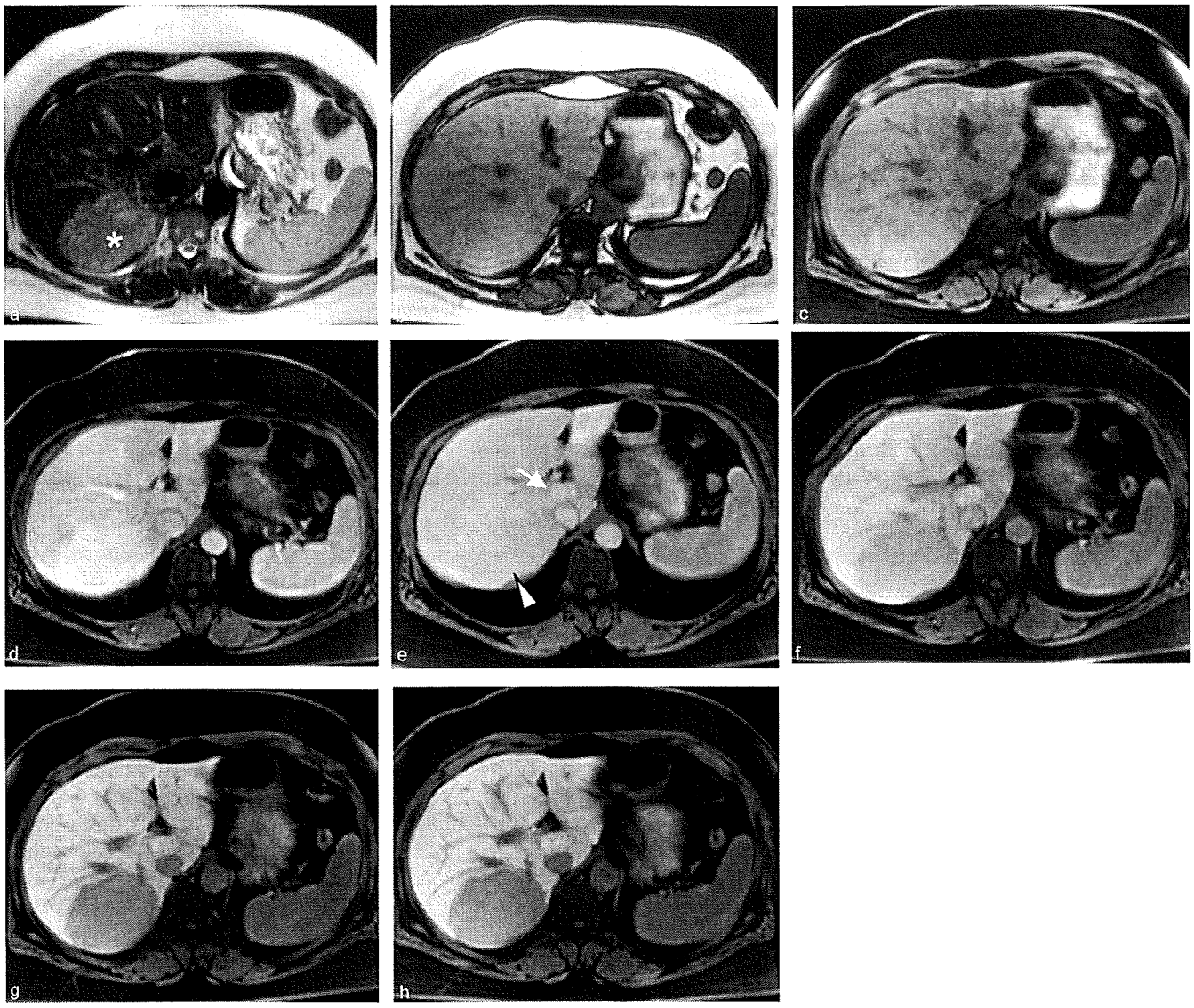

Fig. 2 Appearance of typical hepatic adenoma (and associated FNH) during hepatocyte phase with Gd-EOB-DTPA-enhanced MRI (0.025 mmol/kg body weight). Unenhanced: **a** T2-weighted image, demonstrating large heterogeneous hyperintense lesion at hepatic segment VII (asterisk) and isointense nodule in the segment I. **b** T1-weighted out-phase image, **c** in phase, with both nodules appearing isointense. Dynamic Gd-EOB-DTPA-enhanced T1-weighted images on GRE 3D T1 (VIBE): **d** Arterial phase, both nodules displaying moderate/discrete homogeneous enhancement; portal-venous phase, **e** hepatic adenoma (*arrowhead*) appearing isointense and FNH (*arrow*) tending to be slightly hyperintense; and **f** dynamic late phase, FNH appearing hyperintense whereas hepatic adenoma appearing slightly hypo-intense. Hepatobiliary phase images: **g** 10 min after Gd-EOB-DTPA bolus injection and **h** after 20 min with adenoma appearing hypo-intense and FNH remaining slightly hyperintense

technique to demonstrate true enhancement. Gd-EOB-DTPA-enhanced MRI during the hepatobiliary phase can identify small HCC lesions more clearly than dynamic-phase imaging or dynamic CT due to increased liver-lesion contrast after uptake of Gd-EOB-DTPA by functioning hepatocytes (Fig. 3). The imaging features of hepatocellular nodules in cirrhotic liver should be further explored in future studies.

Consensus statement Gd-EOB-DTPA is highly effective in detecting and staging HCC in the cirrhotic liver. Wash-in and wash-out observed with Gd-EOB-DTPA are highly reproducible. However, additional studies and pathological–radiological correlation are needed. Further studies are also needed to correlate the morphological appearance of Gd-EOB-DTPA-enhanced images in early HCC with patient prognosis.

Table 2 Classification of liver nodules associated with cirrhosis according to Liver Cancer Study Group of Japan

Stage	Type of nodule
1	Large regenerative nodule
2	Low-grade dysplastic nodule
3	High-grade dysplastic nodule
4	Early hepatocellular carcinoma
5	Well differentiated hepatocellular carcinoma (Ed I)
6	Moderately differentiated hepatocellular carcinoma (Ed II)
7	Poorly differentiated hepatocellular carcinoma (Ed III)
8	Undifferentiated hepatocellular carcinoma (Ed IV)

Current diagnostic guidelines

For the non-invasive identification of HCC, the European Association for the Study of the Liver (EASL) [72] and the American Association for the Study of Liver Diseases (AASLD) [73] emphasize the importance of dynamic-phase imaging using MRI and CT to identify hypervascularity. The Japan Society of Hepatology had concerns that the AASLD and EASL recommendations are not necessarily applicable to Japanese patients, and thus published the Consensus-Based Clinical Practice Manual in 2007 [69]. Major differences in the Japanese recommendations compared with EASL and AASLD include the use of two dynamic imaging modalities (e.g. CT and MRI) for the detection of lesions 1–2 cm in diameter (EASL, AASLD) and the use of liver-specific contrast media for the identification of atypical lesions [69] (Japanese recommendations).

Criticisms of current guidelines

There is no lesion-size standardization (AASLD has three categories of lesions: < 1, 1–2 and > 2 cm, each with different diagnostic work-ups) and the definitions of typical and atypical HCC are inconsistent between guidelines. Prevalences vary in different countries; HCC, especially early forms, is particularly high in Japan [74]. This may have a bearing on the advocacy, but usually no justification is provided within the guidelines for a specific recommendation.

There are no differences in the performance of contrast-enhanced helical CT or MRI compared with the more invasive CT hepatic arteriography (CTHA) and CT arterial portography (CTAP) to detect > 2-cm lesions

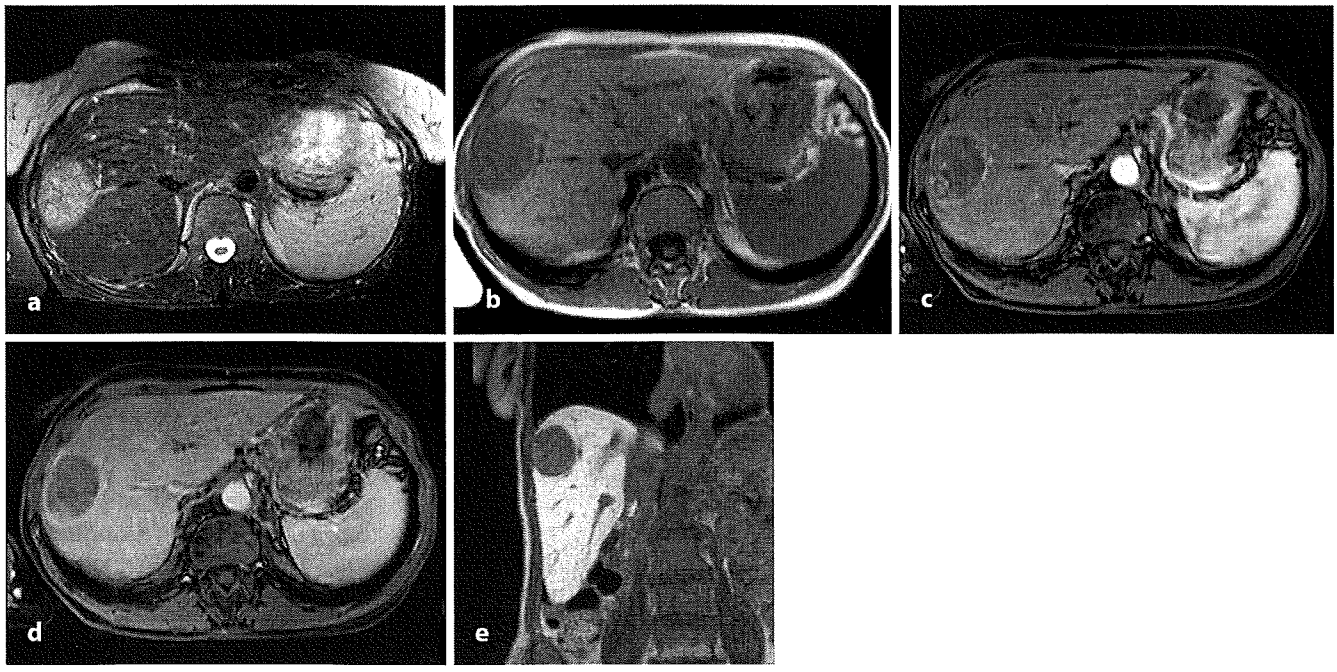

Fig. 3 Appearance of a typical HCC with Gd-EOB-DTPA-enhanced MRI. **a** T2w TSE sequence with respiratory gating. **b** T1w GRE sequence without fat saturation precontrast. **c** 3D VIBE GRE sequence during arterial phase: typical inhomogenous arterial enhancement. **d** 3D VIBE GRE sequence during portalvenous phase: typical portalvenous wash-out. **e** T1w GRE sequence with fat saturation 20 min after injection of Gd-EOB-DTPA: hypointense lesion with high lesion-liver contrast

[75]. Nevertheless, CTHA and CTAP remain in the most recent Japanese guidelines, as well as SPIO-enhanced MRI [69]. A recent innovation is US, using contrast media that enable the simultaneous identification of hypervascularity and the evaluation of Kupffer-cell function [76]. One such contrast medium, which is presently available only in Japan, has been reported to have a diagnostic capability comparable to that of CT [77–79].

Consensus statement The incorporation of an imaging technique within a diagnostic guideline is dependent on sufficient scientific evidence to demonstrate effectiveness. Despite evidence of effectiveness of new techniques, they are yet to be acknowledged.

Evidence for inclusion of Gd-EOB-DTPA-enhanced MRI in diagnostic guidelines

Attendees considered that the diagnostic role of Gd-EOB-DTPA is not fully recognized in the current guidelines. Phase-II and -III trials have demonstrated the effectiveness of Gd-EOB-DTPA in identifying small HCC lesions [18, 19, 23, 24, 26, 71, 80, 81], and this is substantiated by attendees' experiences. Furthermore, data comparing Gd-EOB-DTPA-enhanced MRI with helical CT show that Gd-EOB-DTPA-enhanced MRI is significantly more sensitive in detecting and characterizing focal liver lesions [14, 16, 19, 20, 26]. Studies have also shown that Gd-EOB-DTPA-enhanced MRI is superior to multidetector CT in HCC detection [80, 81] and resulted in fewer false-positive identifications of small lesions compared with helical CT [14].

Consensus statement Clinical studies have demonstrated that Gd-EOB-DTPA-enhanced MRI can detect small HCC lesions better than unenhanced MRI and CT, thus suggesting it has an important place in diagnostic guidelines.

Additional evidence required for the benefit of Gd-EOB-DTPA-enhanced MRI

Multidetector CT has become established as the state-of-the-art modality for abdominal imaging [82]. There are recent data directly comparing Gd-EOB-DTPA-enhanced MRI with multidetector CT [71, 80, 81]. Vogl et al. [24] showed that, compared with Gd-DTPA-enhanced MRI, Gd-EOB-DTPA-enhanced MRI provided improved detection of focal liver lesions. More data, however, are required to show the sensitivity of Gd-EOB-DTPA-enhanced MRI in detecting hypervascular lesions in the presence of liver cirrhosis.

Consensus statement Recent clinical studies have shown the superiority of Gd-EOB-DTPA-enhanced MRI compared with multidetector CT for the visualization and diagnosis of HCC in cirrhosis, although more studies are needed to evaluate the effectiveness of Gd-EOB-DTPA in the presence of liver cirrhosis.

Changes to guidelines

A new, simplified diagnostic algorithm for detection of hyper- and hypovascular liver nodules was developed based on the discussion at the meeting (Fig. 4). The identified criticisms of current guidelines were addressed, and these issues considered when preparing the proposed new guideline. This guideline was considered acceptable to Europe, USA, Australia, Japan, Korea and Thailand.

The proposed guideline place greater emphasis on long-term surveillance of hypovascular lesions, because they can evolve into HCC [83]. Attendees proposed that the term "typical" should be applied to hypervascular lesions with wash-out in the portal-venous phase, whereas an "atypical lesion" would be one that is hypovascular during the arterial phase. Equally, the term could be applied to a lesion that is hypervascular during the arterial phase, but fails to exhibit wash-out in the portal-venous phase. Based on current evidence, atypical lesions require further examination and evaluation by biopsy, but this decision should be made on a case-by-case basis.

Consensus document Based on published data, guidelines on the diagnosis of HCC should be revised to reflect the unique features and benefits of Gd-EOB-DTPA-enhanced MRI.

Gd-EOB-DTPA-enhanced whole-body MRI

Evaluation of rectal cancer patients

Total mesorectal excision (TME) has become the gold standard in many European countries for treating rectal cancer [84]. Tumour, lymph node and metastases (TNM) staging of candidates for TME is time-consuming, involving rectoscopy, endoscopic US, as well as thoracic X-ray in two planes, US of the liver and/or thoracic CT and liver CT to exclude metastases [85]; the multiple imaging techniques can typically take up to 4 working days. The imaging modalities employed are usually determined by the surgeon and can be influenced by funders' re-imbursement policies, which vary considerably in different countries. Conventional MRI has been shown to predict accurately and consistently the circumferential resection margin (CRM) [86,87], an independent prognostic factor for local recurrence of rectal cancer and patient survival. Gd-EOB-DTPA-enhanced MRI is highly effective in detecting liver metastases [14, 19, 23–26, 88, 89].

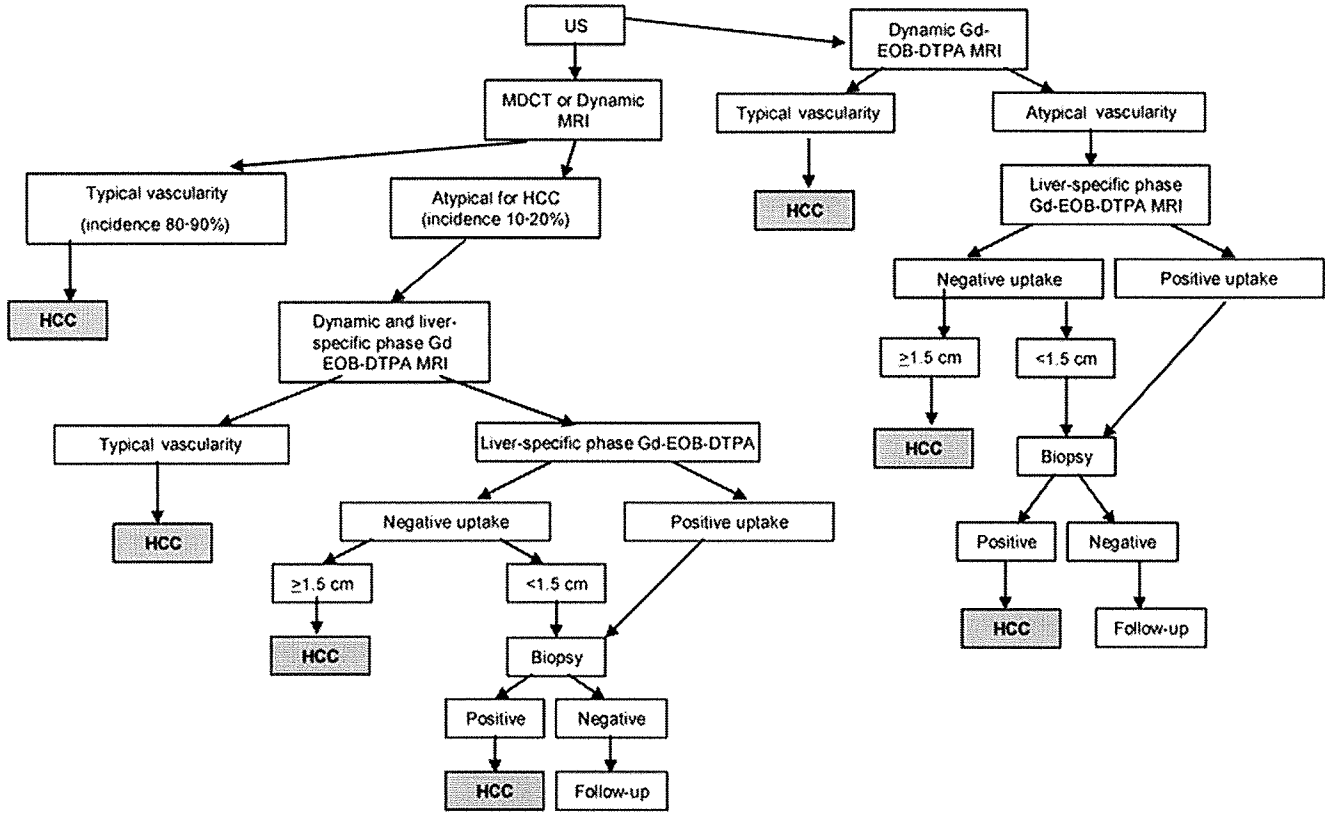

Fig. 4 Proposed revised diagnostic algorithm for hepatocellular carcinoma

The Total Imaging Matrix (Tim®, Siemens Healthcare, Erlangen, Germany) allows contrast-enhanced visualization of the pelvis, abdomen and thorax in a single procedure; the time taken using Gd-EOB-DTPA, employing the proposed protocol (Table 3), is 45–55 min. Consequently, same-day reporting of the findings to an interdisciplinary tumour board is possible, allowing a rapid decision to be made on patient management.

In 12 patients with rectal cancer receiving a mean Gd-EOB-DTPA dose of 0.034 mmol/kg body weight or mean Gd-DTPA dose of 0.1 mmol/kg, overall contrast enhancement was rated sufficient for diagnosis in all examinations with either contrast medium (A. Huppertz, personal communication). Some attendees were concerned about a higher dose of Gd-EOB-DTPA being given in this preliminary study. Clinical studies for registration purposes have demonstrated the excellent safety profile of Primovist at the approved dose of 0.025 mmol/kg body weight [14, 16, 19, 20, 26] ,and limited data are available for higher doses.

A further study of 33 rectal-cancer patients showed that the specificity and sensitivity of Gd-EOB-DTPA-enhanced MRI were greater than those of endoscopic US in determining CRM involvement. Gd-EOB-DTPA-enhanced MRI was also more accurate in identifying lymph node involvement and metastases. With data from multicentre trials supporting the sensitivity and specificity of the procedure, attendees would then feel confident to advise surgeons of the benefits of Gd-EOB-DTPA-enhanced whole-body imaging.

Compared with the time taken for liver imaging, the total time involved for whole-body MRI is relatively long. However, taking all factors into consideration, pharmaco-economic analysis shows that, compared with the current gold-standard diagnostic work-up, Gd-EOB-DTPA-enhanced whole-body MRI reduces the number of investigations and reporting and man-power costs, although hardware and material costs are higher. Overall, the analysis showed that there is a financial saving using Gd-EOB-DTPA-enhanced whole-body MRI (A. Huppertz, personal communication).

The one-stop approach also offers greater convenience for the patient, by not having to wait around between diagnostic procedures if it proves possible to perform more than one on a single day, and having to travel to the hospital on repeated occasions. An improvement in workflow of different hospital departments is also achievable using the whole-body examination. The attendees acknowledged that, in this respect, Gd-EOB-DTPA-enhanced whole-body MRI offers an important advantage not only for the surgeon, but also for the patient.

The availability of a whole-body MRI machine and of staff with expertise in its use are limiting factors. Whole-

Table 3 Proposed whole-body MRI protocol for the TNM staging of rectal cancer. VIBE Volumetric Interpolated Breath-Hold Examination; HASTE Half Fourier Acquisition Single-shot Turbo spin Echo

- Localizer unenhanced pelvis, abdomen and thorax images
- Spasmolysis using intravenous butylscopolamine
- T2-weighted high-resolution imaging of the rectum (axial view)
- Unenhanced T1-weighted imaging of liver (three-dimensional VIBE sequence)
- Bolus injection of Gd-EOB-DTPA (0.035 mmol/kg)
- T1-weighted imaging of liver – arterial phase (three-dimensional VIBE sequence)
- T1-weighted imaging of liver – portal-venous phase (three-dimensional VIBE sequence)
- T1-weighted imaging of thorax – venous phase (three-dimensional VIBE sequence)
- T2-weighted imaging of thorax
- T2-weighted imaging of liver
- Imaging of abdomen (HASTE)
- T1-weighted imaging of liver liver-specific phase (fat saturation)

body MRI has yet to become universally accepted, and the re-imbursement policy of the health-care provider may limit its uptake. However, policies may change if clear financial benefits can be demonstrated.

Consensus statement Preliminary data suggest that the concept of Gd-EOB-DTPA-enhanced whole-body MRI is interesting, and further evaluation is justified. Whole-body MRI offers cost savings, faster diagnosis and greater patient convenience.

Potential of Gd-EOB-DTPA-enhanced whole-body MRI for other malignancies

Other possible uses include evaluation of patients with HCC prior to liver transplantation to confirm the absence of lung metastases [90]. The procedure may also be useful in the regular follow-up of patients with neuro-endocrine carcinomas, although these are admittedly relatively rare. Positron emission tomography combined with CT is increasingly used for this purpose [91], but frequent exposure to radiation may be a concern.

CT colonography is minimally invasive and is now regarded as a relative by inexpensive and reliable diagnostic tool for colon cancer, allowing imaging of the entire colon [92]. Attendees did not envisage that it would be superseded by Gd-EOB-DTPA-enhanced whole-body MRI because of the cost differential. Similarly, Gd-EOB-DTPA-enhanced whole-body MRI is unlikely to be accepted for pancreatic cancer because CT has proven effectiveness and is widely accepted [93]. Because all follow-up examinations should be performed using the same imaging modality [94], whole-body MRI would probably be inappropriate for patients with pancreatic cancer, who would almost certainly have been originally examined using CT. Gd-EOB-DTPA whole-body MRI would seem to provide no advantage in the diagnosis of prostatic cancer, for which a multidisciplinary approach of a combination of prostate-specific antigen testing, skeletal scintigraphy and CT staging is regarded as the gold standard [95]. For the primary diagnosis of breast cancer, dedicated breast CT machines are rapidly gaining acceptance [96]. Dedicated MRI breast coils could currently not be used in conjunction with whole-body MRI machines. In addition, the approach to the staging of breast cancer differs from that used for rectal cancer. A whole-body MR examination is not justified when the sentinel nodes are negative.

Consensus statement Other potential uses of Gd-EOB-DTPA-enhanced whole-body MRI are the evaluation of potential liver transplant candidates and in the follow-up of patients with neuro-endocrine tumours.

Conclusions

Gd-EOB-DTPA, a hepatocyte-specific contrast agent with unique pharmacokinetic features, addresses many of the challenges that radiologists face when seeking high-sensitivity and accurate imaging of the liver for the identification of focal liver lesions. The high ability to detect lesions < 1 cm in diameter distinguishes Gd-EOB-DTPA-enhanced liver MRI from CT. Images obtained during the dynamic arterial, portal-venous and late phases, together with those gathered during the hepatocyte-specific phase, allow the characterization of both benign and malignant lesions on the basis of lesion vascularity and the hepatocyte content with high diagnostic confidence in both the non-cirrhotic and cirrhotic patient using a single procedure. Thus, Gd-EOB-DTPA-enhanced MRI has an important role in the planning of the management of patients with benign lesions, the monitoring of precancerous changes and the identification of HCC. The benefits of Gd-EOB-DTPA should be recognized with its inclusion in future diagnostic algorithms for the evaluation of liver nodules, replacing more invasive imaging techniques such as CTHA and CTAP. The full potential of Gd-EOB-DTPA has to be further established. Initial studies suggest that Gd-EOB-DTPA is not only a powerful tool in liver imaging, but may also allow one-stop, whole-body imaging for the simultaneous detection of primary lesions in, for example, the rectum as well as lung and liver metastases and assist in the identification of liver transplant candidates.

Conflict of interest: This work was funded by Bayer Schering Pharma AG, Berlin, Germany.

References

1. Ba-Ssalamah A, Uffmann M, Saini S, Bastati N, Herold C, Schima W (2009) Clinical value of MRI liver-specific contrast agents: a tailored examination for a confident non-invasive diagnosis of focal liver lesions. Eur Radiol 19:342–357
2. Reimer P, Schneider G, Schima W (2004) Hepatobiliary contrast agents for contrast-enhanced MRI of the liver: properties, clinical development and applications. Eur Radiol 14:559–578
3. Weinmann HJ, Schuhmann-Giampieri G, Schmitt-Willich H, Vogler H, Frenzel T, Gries H (1991) A new lipophilic gadolinium chelate as a tissue-specific contrast medium for MRI. Magn Reson Med 22:233–237
4. Hamm B, Staks T, Mühler A, Bollow M, Taupitz M, Frenzel T, Wolf KJ, Weinmann HJ, Lange L (1995) Phase I clinical evaluation of Gd-EOB-DTPA as a hepatobiliary MR contrast agent: safety, pharmacokinetics, and MR imaging. Radiology 195:785–792
5. Shuter B, Tofts PS, Wang SC, Pope JM (1996) The relaxivity of Gd-EOB-DTPA and Gd-DTPA in liver and kidney of the Wistar rat. Magn Reson Imaging 14:243–253
6. Rohrer M, Bauer H, Mintorovitch J, Requardt M, Weinmann HJ (2005) Comparison of magnetic properties of MRI contrast media solutions at different magnetic field strengths. Invest Radiol 40:715–724
7. Vander Elst L, Maton F, Laurent S, Seghi F, Chapelle F, Muller RN (1997) A multinuclear MR study of Gd-EOB-DTPA: comprehensive preclinical characterization of an organ-specific MRI contrast agent. Magn Reson Med 38:604–614
8. Murakami T, Kim T, Oi H, Nakamura H, Igarashi H, Matsushita M, Okamura J, Kozuka T (1995) Detectability of hypervascular hepatocellular carcinoma by arterial phase images of MR and spiral CT. Acta Radiol 36:372–376
9. Malone D, Zech CJ, Ayuso C, Bartolozzi C, Jonas E, Tanimoto A (2008) Magnetic resonance imaging of the liver: consensus statement of the 1st Primovist User Meeting. Eur Radiol Suppl 18:849–864
10. Goudemant JF, Van Beers BE, Demeure R, Grandin C, Delos M, Pringot J (1998) Comparison of unenhanced and gadoxetate disodium-enhanced spin-echo magnetic resonance imaging for the detection of experimental hepatocellular carcinoma in the rat. Invest Radiol 33:80-84
11. Khangure MS, Hua J (1996) Comparative assessment of gadoxetate disodium, manganese dipyridoxal diphosphate, and superparamagnetic iron oxide for enhancement of the liver in dogs. Acad Radiol 3(Suppl 2): S458–S460
12. Schmitz SA, Mühler A, Wagner S, Wolf KJ (1996) Functional hepatobiliary imaging with gadolinium-EOB-DTPA. A comparison of magnetic resonance imaging and ^{153}gadolinium-EOB-DTPA scintigraphy in rats. Invest Radiol 31:154–160
13. Segers J, Le Duc G, Laumonier C, Troprès I, Elst LV, Muller RN (2005) Evaluation of Gd-EOB-DTPA uptake in a perfused and isolated mouse liver model: correlation between magnetic resonance imaging and monochromatic quantitative computed tomography. Invest Radiol 40:574–582
14. Bluemke DA, Sahani D, Amendola M, Balzer T, Breuer J, Brown JJ, Casalino DD, Davis PL, Francis IR, Krinsky G, Lee FT Jr, Lu D, Paulson EK, Schwartz LH, Siegelman ES, Small WC, Weber TM, Welber A, Shamsi K (2005) Efficacy and safety of MR imaging with liver-specific contrast agent: U.S. multicenter phase-III study. Radiology 237:89–98
15. Dahlström N, Persson A, Albiin N, Smedby O, Brismar TB (2007) Contrast-enhanced magnetic resonance cholangiography with Gd-BOPTA and Gd-EOB-DTPA in healthy subjects. Acta Radiol 48:362–368
16. Halavaara J, Breuer J, Ayuso C, Balzer T, Bellin MF, Blomqvist L, Carter R, Grazioli L, Hammerstingl R, Huppertz A, Jung G, Krause D, Laghi A, Leen E, Lupatelli L, Marsili L, Martin J, Pretorius ES, Reinhold C, Stiskal M, Stolpen AH (2006) Liver tumor characterization: comparison between liver-specific gadoxetic acid disodium-enhanced MRI and biphasic CT – a multicenter trial. J Comput Assist Tomogr 30:345–354
17. Hamm B, Thoeni RF, Gould RG, Bernardino ME, Lüning M, Saini S, Mahfouz AE, Taupitz M, Wolf KJ (1994) Focal liver lesions: characterization with nonenhanced and dynamic contrast material-enhanced MR imaging. Radiology 190:417–423
18. Hammerstingl R, Zangos S, Schwarz W, Rosen T, Bechstein WO, Balzer T, Vogl TJ (2002) Contrast-enhanced MRI of focal liver tumors using a hepatobiliary MR contrast agent: detection and differential diagnosis using Gd-EOB-DTPA-enhanced versus Gd-DTPA-enhanced MRI in the same patient. Acad Radiol 9(Suppl 1):S119–S120
19. Huppertz A, Balzer T, Blakeborough A, Breuer J, Giovagnoni A, Heinz-Peer G, Laniado M, Manfredi RM, Mathieu DG, Mueller D, Reimer P, Robinson PJ, Strotzer M, Taupitz M, Vogl TJ; European EOB Study Group (2004) Improved detection of focal liver lesions at MR imaging: multicenter comparison of gadoxetic acid-enhanced MR images with intraoperative findings. Radiology 230:266–275
20. Huppertz A, Haraida S, Kraus A, Zech CJ, Scheidler J, Breuer J, Helmberger TK, Reiser MF (2005) Enhancement of focal liver lesions at gadoxetic acid-enhanced MR imaging: correlation with histopathologic findings and spiral CT – initial observations. Radiology 234:468–478
21. Kacl GM, Hagspiel KD, Marincek B (1997) Focal nodular hyperplasia of the liver: serial MRI with Gd-DOTA, superparamagnetic iron oxide, and Gd-EOB-DTPA. Abdom Imaging 22:264–267
22. Reimer P, Rummeny EJ, Shamsi K, Balzer T, Daldrup HE, Tombach B, Hesse T, Berns T, Peters PE (1996) Phase II clinical evaluation of Gd-EOB-DTPA: dose, safety aspects, and pulse sequence. Radiology 199:177–183
23. Reimer P, Rummeny EJ, Daldrup HE, Hesse T, Balzer T, Tombach B, Peters PE (1997) Enhancement characteristics of liver metastases, hepatocellular carcinomas, and hemangiomas with Gd-EOB-DTPA: preliminary results with dynamic MR imaging. Eur Radiol 7:275–280
24. Vogl TJ, Kümmel S, Hammerstingl R, Schellenbeck M, Schumacher G, Balzer T, Schwarz W, Müller PK, Bechstein WO, Mack MG, Söllner O, Felix R (1996) Liver tumors: comparison of MR imaging with Gd-EOB-DTPA and Gd-DTPA. Radiology 200:59–67
25. Zech CJ, Herrmann KA, Reiser MF, Schoenberg SO (2007) MR imaging in patients with suspected liver metastases: value of liver-specific contrast agent Gd-EOB-DTPA. Magn Reson Med Sci 6:43–52
26. Hammerstingl R, Huppertz A, Breuer J, Balzer T, Blakeborough A, Carter R, Fusté LC, Heinz-Peer G, Judmaier W, Laniado M, Manfredi RM, Mathieu DG, Müller D, Mortelè K, Reimer P, Reiser MF, Robinson PJ, Shamsi K, Strotzer M, Taupitz M, Tombach B, Valeri G, van Beers BE, Vogl TJ; European EOB-study group (2008) Diagnostic efficacy of gadoxetic acid (Primovist)-enhanced MRI and spiral CT for a therapeutic strategy:

comparison with intraoperative and histopathologic findings in focal liver lesions. Eur Radiol 18:457–467
27. Bae KT, Heiken JP, Brink JA (1998) Aortic and hepatic peak enhancement at CT: effect of contrast medium injection rate–pharmacokinetic analysis and experimental porcine model. Radiology 206:455–464
28. Prince MR (1994) Gadolinium-enhanced MR aortography. Radiology 191:155–164
29. Shinozaki K, Yoshimitsu K, Irie H, Aibe H, Tajima T, Nishie A, Nakayama T, Kakihara D, Shimada M, Honda H (2004) Comparison of test-injection method and fixed-time method for depiction of hepatocellular carcinoma using dynamic steady-state free precession magnetic resonance imaging. J Comput Assist Tomogr 28:628–634
30. Foo TK, Saranathan M, Prince MR, Chenevert TL (1997) Automated detection of bolus arrival and initiation of data acquisition in fast, three-dimensional, gadolinium-enhanced MR angiography. Radiology 203:275–280
31. Prince MR, Chenevert TL, Foo TK, Londy FJ, Ward JS, Maki JH (1997) Contrast-enhanced abdominal MR angiography: optimization of imaging delay time by automating the detection of contrast material arrival in the aorta. Radiology 203:109–114
32. Ho VB, Foo TK (1998) Optimization of gadolinium–enhanced magnetic resonance angiography using an automated bolus-detection algorithm (MR SmartPrep). Original investigation. Invest Radiol 33:515–523
33. Riedy G, Golay X, Melhem ER (2005) Three-dimensional isotropic contrast-enhanced MR angiography of the carotid artery using sensitivity-encoding and random elliptic centric k-space filling: technique optimization. Neuroradiology 47:668–673
34. Svensson J, Petersson JS, Ståhlberg F, Larsson EM, Leander P, Olsson LE (1999) Image artefacts due to a time-varying contrast medium concentration in 3D contrast-enhanced MRA. Magn Reson Imaging 10:919–928
35. Maki JH, Prince MR, Londy FJ, Chenevert TL (1996) The effects of time varying intravascular signal intensity and k-space acquisition order on three-dimensional MR angiography image quality. J Magn Reson Imaging 6:642–651
36 Carr JC, Nemcek AA Jr, Abecassis M, Blei A, Clarke L, Pereles FS, McCarthy R, Finn JP (2003) Preoperative evaluation of the entire hepatic vasculature in living liver donors with use of contrast-enhanced MR angiography and true fast imaging with steady-state precession. J Vasc Interv Radiol 14:441–44937
37. Zech CJ, Vos B, Nordell A, Urich M, Blomqvist L, Breuer J, Reiser MF, Weinmann HJ (2009) Vascular enhancement in early dynamic liver MR imaging in an animal model: comparison of two injection regimen and two different doses Gd-EOB-DTPA (gadoxetic acid) with standard Gd-DTPA. Invest Radiol 44:305–310
38. Hany TF, McKinnon GC, Leung DA, Pfammatter T, Debatin JF (1997) Optimization of contrast timing for breath-hold three-dimensional MR angiography. J Magn Reson Imaging 7:551–556
39. Dorio PJ, Lee FT Jr, Henseler KP, Pilot M, Pozniak MA, Winter TC 3rd, Shock SA (2003) Using a saline chaser to decrease contrast media in abdominal CT. AJR Am J Roentgenol 180:929–934
40. Haage P, Schmitz-Rode T, Hübner D, Piroth W, Günther RW (2000) Reduction of contrast material dose and artefacts by a saline flush using a double power injector in helical CT of the thorax. AJR Am J Roentgenol 174:1049–1053
41. Orlandini F, Boini S, Iochum-Duchamps S, Batch T, Zhu X, Blum A (2005) Assessment of the use of a saline chaser to reduce the volume of contrast medium in abdominal CT. AJR Am J Roentgenol 187:511–515
42. Saini, S; Nelson, RC (1995) Technique for MR imaging of the liver. Radiology 197:575–577
43. Kim T, Murakami T, Hasuike Y, Gotoh M, Kato N, Takahashi M, Miyazawa T, Narumi Y, Monden M, Nakamura H (1997) Experimental hepatic dysfunction: evaluation by MRI with Gd-EOB-DTPA. J Magn Reson Imaging 7:683–688
44. Runge VM (1998) A comparison of two MR hepatobiliary gadolinium chelates: Gd-BOPTA and Gd-EOB-DTPA. J Comput Assist Tomogr 22:643–650
45. Tschirch FT, Struwe A, Petrowsky H, Kakales I, Marincek B, Weishaupt D (2008) Contrast-enhanced MR cholangiography with Gd-EOB-DTPA in patients with liver cirrhosis: visualization of the biliary ducts in comparison with patients with normal liver parenchyma. Eur Radiol 18:1577–1586
46. Rofsky NM, Weinreb JC, Ambrosino MM, Safir J, Krinsky G (1996) Comparison between in-phase and opposed-phase T1-weighted breath-hold FLASH sequences for hepatic imaging. J Comput Assist Tomogr 20:230–235
47. Namasivayam S, Martin DR, Saini S (2007) Imaging of liver metastases: MRI. Cancer Imaging 7:2–9
48. Tanimoto A, Yuasa Y, Jinzaki M, Nakatsuka S, Takeda T, Kurata T, Shinmoto H, Kuribayashi S (2002) Routine MR imaging protocol with breath-hold fast scans: diagnostic efficacy for focal liver lesions. Radiat Med 20:169–179
49. Ramalho M, Altun E, Herédia V, Zapparoli M, Semelka R (2007) Liver MR imaging: 1.5T versus 3T. Magn Reson Imaging Clin N Am 15:321–347
50. Schindera ST, Merkle EM, Dale BM, Delong DM, Nelson RC (2006) Abdominal magnetic resonance imaging at 3.0 T. What is the ultimate gain in signal-to-noise ratio? Acad Radiol 13:1236–1243
51. von Falkenhausen MM, Lutterbey G, Morakkabati-Spitz N, Walter O, Gieseke J, Blömer R, Willinek WA, Schild HH, Kuhl CK (2006) High-field-strength MR imaging of the liver at 3.0 T: intraindividual comparative study with MR imaging at 1.5 T. Radiology 241:156–166
52. Tsurusaki M, Semelka RC, Zapparoli M, Elias J Jr, Altun E, Pamuklar E, Sugimura K (2008) Quantitative and qualitative comparison of 3.0T and 1.5T MR imaging of the liver in patients with diffuse parenchymal liver disease. Eur J Radiol Sep 12
53. Asbach P, Warmuth C, Stemmer A, Rief M, Huppertz A, Hamm B, Taupitz M, Klessen C (2008) High spatial resolution T1-weighted MR imaging of liver and biliary tract during uptake phase of a hepatocyte-specific contrast medium. Invest Radiol 43:809–915
54. Casarella WJ, Knowles DM, wolff M, Johnson PM (1978) Focal nodular hyperplasia and liver cell adenoma: radiologic and pathologic differentiation. AJR Am J Roentgenol 131:393–402
55. Paradis V, Benzekri A, Dargère D, Bièche I, Laurendeau I, Vilgrain V, Belghiti J, Vidaud M, Degott C, Bedossa P (2004) Telangiectatic focal nodular hyperplasia: a variant of hepatocellular adenoma. Gastroenterology 126:1323–1329
56. Mortelé KJ, Praet M, Van Vlierberghe H, Kunnen M, Ros PR (2000) CT and MR imaging findings in focal nodular hyperplasia of the liver: radiologic–pathologic correlation. AJR Am J Roentgenol 175:687–692
57. Zech CJ, Grazioli L, Breuer J, Reiser MF, Schoenberg SO (2008) Diagnostic performance and description of morphological features of focal nodular hyperplasia in Gd-EOB-DTPA-enhanced liver magnetic resonance imaging: results of a multicenter trial. Invest Radiol 43:504–511

58. Giovagnoli O, Hein M, Terracciano L, Bongartz G, Ledermann HP (2008) MRI of hepatic adenomatosis: initial observations with gadoxetic acid contrast agent in three patients. AJR 190:W290-W293
59. Grazioli L, Morana G, Kirchin MA, Schneider G. (2005) Accurate differentiation of focal nodular hyperplasia from hepatic adenoma at gadobenate dimeglumine-enhanced MR imaging: prospective study. Radiology 236:166–177
60. Oudkerk M, Torres CG, Song B, König M, Grimm J, Fernandez-Cuadrado J, Op de Beeck B, Marquardt M, van Dijk P, de Groot JC (2002) Characterization of liver lesions with mangafodipir trisodium-enhanced MR imaging: multicenter study comparing MR and dual-phase spiral CT. Radiology 223:517–524
61. Matsui O, Kadoya M, Kameyama T, Yoshikawa J, Takashima T, Nakanuma Y, Unoura M, Kobayashi K, Izumi R, Ida M, Kitagawa K (1991) Benign and malignant nodules in cirrhotic livers: distinction based on blood supply. Radiology 178:493–497
62. Hayashi M, Matsui O, Ueda K, Kawamori Y, Kadoya M, Yoshikawa J, Gabata T, Takashima T, Nonomura A, Nakanuma Y (1999) Correlation between the blood supply and grade of malignancy of hepatocellular nodules associated with liver cirrhosis: evaluation by CT during intraarterial injection of contrast medium. AJR Am J Roentgenol 172:969–976
63. Matsui O, Kadoya M, Kameyama T, Yoshikawa J, Arai K, Gabata T, Takashima T, Nakanuma Y, Terada T, Ida M (1989) Adenomatous hyperplastic nodules in the cirrhotic liver: differentiation from hepatocellular carcinoma with MR imaging. Radiology 173:123–126
64. Imai Y, Murakami T, Yoshida S, Nishikawa M, Ohsawa M, Tokunaga K, Murata M, Shibata K, Zushi S, Kurokawa M, Yonezawa T, Kawata S, Takamura M, Nagano H, Sakon M, Monden M, Wakasa K, Nakamura H (2000) Superparamagnetic iron oxide-enhanced magnetic resonance images of hepatocellular carcinoma: correlation with histological grading. Hepatology 32:205–212
65. Lim JH, Choi D, Cho SK, Kim SH, Lee WJ, Lim HK, Park CK, Paik SW, Kim YI (2001) Conspicuity of hepatocellular nodular lesions in cirrhotic livers at ferumoxides-enhanced MR imaging: importance of Kupffer cell number. Radiology 220:669–676
66. Suzuki S, Iijima H, Moriyasu F, Sasaki S, Yanagisawa K, Miyahara T, Oguma K, Yoshida M, Horibe T, Ito N, Kakizaki D, Abe K, Tsuchiya K (2004) Differential diagnosis of hepatic nodules using delayed parenchymal phase imaging of Levovist contrast ultrasound: comparative study with SPIO-MRI. Hepatol Res 29:122–126
67. Lim JH, Lee SJ, Lee WJ, Lim HK, Choo SW, Choo IW (1999) Iodized oil retention due to postbiopsy arterioportal shunt: a false positive lesion in the investigation of hepatocellular carcinoma. Abdom Imaging 24:165–170
68. Peterson MS, Baron RL, Marsh JW Jr, Oliver JH 3rd, Confer SR, Hunt LE (2000) Pretransplantation surveillance for possible hepatocellular carcinoma in patients with cirrhosis: epidemiology and CT-based tumor detection rate in 430 cases with surgical pathologic correlation. Radiology 217:743–749
69. Kudo M, Okanoue T; Japan Society of Hepatology (2007) Management of hepatocellular carcinoma in Japan: consensus-based clinical practice manual proposed by the Japan Society of Hepatology. Oncology 72(Suppl 1):2–15
70. Roncalli M, Borzio M, Di Tommaso L (2008) Hepatocellular dysplastic nodules. Ann Ital Chir 79:81–89
71. di Martino M, Marin D, Guerrisi A, Geiger D, Galati F, Catalano C (2008) Detection of hepatocellular carcinoma (HCC) in patients with cirrhosis: intraindividual comparison of gadoxetic acid (GD-EOB-DTPA)-enhanced MR imaging and multiphasic 64-slice CT [abstract ssa07-07]. Radiological Society of North America
72. Bruix J, Sherman M, Llovet JM, Beaugrand M, Lencioni R, Burroughs AK, Christensen E, Pagliaro L, Colombo M, Rodés J; EASL Panel of Experts on HCC. Clinical management of hepatocellular carcinoma (2001). Conclusions of the Barcelona – 2000 EASL conference. J Hepatol 35:421–430
73. Bruix J, Sherman M; Practice Guidelines Committee, American Association for the Study of Liver Diseases (2005) Management of hepatocellular carcinoma. Hepatology 42:1208–1236
74. Okita K (2006) Clinical aspects of hepatocellular carcinoma in Japan. Intern Med 45:229–233
75. Hori M, Murakami T, Oi H, Kim T, Takahashi S, Matsushita M, Tomoda K, Narumi Y, Kadowaki K, Nakamura H (1998) Sensitivity in detection of hypervascular hepatocellular carcinoma by helical CT with intra-arterial injection of contrast medium, and by helical CT and MR imaging with intravenous injection of contrast medium. Acta Radiol 39:144–151
76. Sontum PC (2008) Physicochemical characteristics of Sonazoid, a new contrast agent for ultrasound imaging. Ultrasound Med Biol 34:824–833
77. Hatanaka K, Kudo M, Minami Y, Ueda T, Tatsumi C, Kitai S, Takahashi S, Inoue T, Hagiwara S, Chung H, Ueshima K, Maekawa K (2008) Differential diagnosis of hepatic tumors: value of contrast-enhanced harmonic sonography using the newly developed contrast agent, Sonazoid. Intervirology 51(Suppl 1):61–69
78. Maruyama H, Takahashi M, Ishibashi H, Okugawa H, Okabe S, Yoshikawa M, Yokosuka O (2008) Ultrasound-guided treatments under low acoustic power contrast harmonic imaging for hepatocellular carcinomas undetected by B-mode ultrasonography. Liver Int Sep 18
79. Luo W, Numata K, Morimoto M, Nozaki A, Nagano Y, Sugimori K, Zhou X, Tanaka K (2008) Clinical utility of contrast-enhanced three-dimensional ultrasound imaging with Sonazoid: findings on hepatocellular carcinoma lesions. Eur J Radiol Oct 17
80. di Martino M, Marin D, Guerrisi A, Geiger D, Catalano C, Passariello R (2009) Intraindividual comparison of gadoxetic acid (Gd-EOB-DTPA) enhanced MR imaging and multiphasic 64-slice CT for the detection of hepatocellular carcinoma (HCC) in patients with cirrhosis [abstract B-096]. Proceedings of the European Congress of Radiology, Vienna, Austria
81. Kim SH, Kim SH, Lee J, Kim MJ, Jeon YH, Park Y, Choi D, Lee WJ, Lim HK (2009) Gadoxetic acid-enhanced MRI versus triple-phase MDCT for the preoperative detection of hepatocellular carcinoma. AJR Am J Roentgenol 192:1675–161
82. Harris JP, Nelson RC (2004) Abdominal Imaging with multidetector computed tomography: State of the art. J Comput Assist Tomogr 28(Suppl 1): S17–S19
83. Leoni S, Piscaglia F, Righini R, Bolondi L (2006) Management of small hepatocellular carcinoma. Acta Gastroenterol Belg 69:230–235
84. Ridgway PE, Darzi AW (2003) The role of total mesorectal excision in the management of rectal cancer. Cancer Control 10:205–211
85. Engelen SM, Beets GL, Beets-Tan RG (2007) Role of preoperative local and distant staging in rectal cancer. Onkologie 30:141–145
86. Beets-Tan RG, Beets GL, Vliegen RF, Kessels AG, Van Boven H, De Bruine A, von Meyenfeldt MF, Baeten CG, van Engelshoven JM (2001) Accuracy of magnetic resonance imaging in prediction of tumour-free resection

margin in rectal cancer surgery. Lancet 357:497–504
87. Oberholzer K, Junginger T, Kreitner KF, Krummenauer F, Simiantonaki N, Trouet S, Thelen M (2005) Local staging of rectal carcinoma and assessment of the circumferential resection margin with high–resolution MRI using an integrated parallel acquisition technique. J Magn Reson Imaging 22:101–108
88 Mühler A, Clément O, Vexler V, Berthezène Y, Rosenau W, Brasch RC (1992) Hepatobiliary enhancement with Gd-EOB-DTPA: comparison of spin-echo and STIR imaging for detection of experimental liver metastases. Radiology 184:207–213
89. Stern W, Schick F, Kopp AF, Reimer P, Shamsi K, Claussen CD, Laniado M (2000) Dynamic MR imaging of liver metastases with Gd-EOB-DTPA. Acta Radiol 41:255–262
90. Ferris JV, Marsh JW, Little AF (1995) Presurgical evaluation of the liver transplant candidate. Radiol Clin North Am 33:497–520
91. Rosenbaum SJ, Stergar H, Antoch G, Veit P, Bockisch A, Kühl H (2006) Staging and follow-up of gastrointestinal tumors with PET/CT. Abdom Imaging 31:25–35
92. Mang T, Graser A, Schima W, Maier A (2007) CT colonography: techniques, indications, findings. Eur J Radiol 61:388–399
93. Tunaci M (2004) Multidetector row CT of the pancreas. Eur J Radiol 52:18–30
94. Freelove R, Walling AD (2006) Pancreatic cancer: diagnosis and management. Am Fam Physician 73:485–492
95. Hricak H, Choyke PL, Eberhardt SC, Leibel SA, Scardino PT (2007) Imaging prostate cancer: a multidisciplinary perspective. Radiology 243:28–53
96. Glick SJ (2007) Breast CT. Annu Rev Biomed Eng 9:501–526

Percutaneous Aspiration and Ethanolamine Oleate Sclerotherapy for Sustained Resolution of Symptomatic Polycystic Liver Disease: An Initial Experience

Ryosuke Nakaoka[1]
Kunal Das[1,2]
Masatoshi Kudo[1]
Hobyung Chung[1]
Tatsuo Innoue[1]

OBJECTIVE. Surgical therapy for symptomatic polycystic liver disease is effective but has substantial mortality and morbidity. Minimally invasive options such as percutaneous aspiration with or without ethanol sclerosis have had disappointing results. The purpose of this study was to evaluate percutaneous aspiration with ethanolamine oleate sclerosis in the management of symptomatic polycystic liver disease.

SUBJECTS AND METHODS. The study included 13 patients (11 with polycystic liver disease, two with simple cysts) with 17 cysts. All patients underwent percutaneous aspiration of the liver cyst under ultrasound guidance followed by insertion of a 7-French pigtail catheter, instillation of ethanolamine oleate (10% of cyst volume), and aspiration of the ethanolamine oleate. The catheter was kept in place for 24 hours of open drainage and then removed.

RESULTS. All but one of the cysts resolved with one instillation. The one cyst, in a patient with polycystic liver disease, required two instillations 3 months apart. The mean initial volume of cysts was 589.8 mL, and the mean reduction in volume was 88.8%. Both the simple cysts resolved completely. In the cases of polycystic disease, the volume of cysts larger than 10 cm in diameter was reduced by 92.8%. Cyst resolution was gradual, and clinically significant cyst reduction was achieved within 1 year of therapy. None of the patients needed surgery. The median follow-up period was 54 months (range, 1 week–95 months). There were no significant adverse effects, and all patients had relief of symptoms after therapy.

CONCLUSION. This initial experience with a single session of percutaneous aspiration and ethanolamine oleate sclerosis resulted in sustained resolution of symptomatic polycystic liver disease with minimal morbidity, avoidance of surgery, and improvement in quality of life.

Keywords: ethanol sclerosis, ethanolamine oleate, hepatic cysts, polycystic liver disease, sclerotherapy

DOI:10.2214/AJR.08.1681

Received August 17, 2008; accepted after revision May 18, 2009.

[1]Department of Gastroenterology and Hepatology, Kinki University School of Medicine, 377-2 Onho-Higashi, Osaka-sayama, Osaka, Japan. Address correspondence to M. Kudo.

[2]Department of Gastroenterology and Hepatology, Fortis Hospital, Noida, Uttar Pradesh, India.

AJR 2009; 193:1540–1545

0361–803X/09/1936–1540

The management of polycystic liver disease (PLD) is notoriously difficult and challenging. Symptomatic cysts first require careful differential diagnosis from cystadenoma, cystadenocarcinoma, and hepatic metastasis. Symptoms can be attributed to hepatic cysts after exclusion of biliary colic, gallstones, reflux disease, peptic ulcer, nonulcer dyspepsia, chronic pancreatitis, and irritable bowel syndrome as potential causes of symptoms [1]. Most patients have no symptoms, but the minority who do have symptoms need to be considered for treatment.

Management options for PLD include needle aspiration with or without injection of a sclerosing solution, internal drainage with cystojejunostomy, deroofing of the cyst by open laparotomy or laparoscopy, varying degrees of liver resection, liver transplantation, and hepatic arterial embolization [2, 3]. Percutaneous ultrasound- or CT-guided needle aspiration of hepatic cysts has a high recurrence rate (78–100%) due to the presence of epithelial cell lining [4, 5]. Percutaneous aspiration and ethanol sclerosis for PLD is largely useless because of a high recurrence rate, greater than 75% [1, 6]. The procedure is generally safe and effective in the management of solitary cysts, however, and is associated with a low recurrence rate in that circumstance [6]. Alcohol destroys the cells lining the cyst cavity, disabling cystic fluid secretion [7] and resulting in cyst resolution. Ethanol injected as a sclerosing agent after aspiration of the cyst contents can cause complications if it leaks from a cyst or is systemically absorbed [8]. Therefore, percutaneous sclerosis has been attempted with other substances, such as iophendylate [9], tetracycline chloride [10], doxycycline [11], minocycline chloride [12], and hypertonic saline solution [13]. The surgical options, including

laparoscopic deroofing with or without hepatic resection and liver transplantation, are effective but have substantial morbidity and mortality and require technical expertise. Surgery therefore is reserved for the few selected cases caused by one or a few dominant cysts superficially located in anterior segments of the right hepatic lobe [14].

Ethanolamine oleate has been used with immense success in sclerotherapy for esophageal varices [15]. Like alcohol, ethanolamine oleate destroys the cystic epithelial cells immediately, bringing about cyst resolution [16]. In a study with a small number of subjects [17], ethanolamine oleate was used successfully for sclerosis of simple hepatic and renal cysts. To our knowledge, in no previous study has ethanolamine oleate been used in sclerotherapy for PLD. Ethanolamine oleate sclerosis is minimally invasive; if it is successful, surgery can be avoided and the quality of life of patients improved. The purpose of this study was to evaluate the usefulness of percutaneous aspiration and ethanolamine oleate sclerosis of symptomatic hepatic cysts, most of which were associated with PLD.

Subjects and Methods

All patients gave a written consent for the study, and the study protocol was approved by the ethics committee at our institution. From June 1998 through June 2007, all patients consecutively referred to our department with symptomatic liver cysts were included in this prospective study. These 13 patients (10 women, three men) had 17 cysts. The symptomatic liver cysts were classified into two groups: simple solitary or multiple liver cysts or cysts of PLD. The latter included autosomal dominant PLD and PLD in the presence of polycystic kidney disease.

Simple liver cysts typically were visualized on ultrasound images [18] as anechoic smooth borders with strong posterior echo enhancement and an accentuation of echoes beyond the cyst wall. On CT scans, simple liver cysts appeared as well-demarcated lesions with fluid attenuation and without enhancement after contrast administration. The cysts of PLD typically appeared as multiple homogeneous lesions with fluid attenuation and without wall or content enhancement after IV contrast administration [19]. The volume of the cyst was estimated as the volume of an ellipse, as suggested previously [16].

The procedure was performed on an inpatient basis. The puncture site, needle angle, and depth were chosen in real time at sonography. In patients with multicystic disease, the cyst most probably responsible for the symptoms was chosen for treatment according to location and size. After antiseptic preparation of the skin and local anesthesia with lidocaine, the cyst was punctured with an 18-gauge percutaneous transhepatic aspiration needle. A guidewire was inserted, and a 7-French single pigtail catheter was placed over the guidewire. As much as possible of the contents of the cyst were aspirated, and the cystic fluid was sent for cytologic and bacteriologic examination.

To avoid leakage of ethanolamine oleate, a puncture line traversing normal liver parenchyma was determined. The cyst was opacified by injection of contrast medium to verify the absence of communication between the cyst cavity and the biliary tree and of leak to the peritoneal cavity, urinary tract, or surrounding hepatic vessels. The amount of contrast medium injected was the same as the volume aspirated from the cyst cavity (Table 1).

During cystography in this study, no vessel, bile duct, or urinary structure was visible before ethanolamine oleate sclerosis. In such a situation, percutaneous aspiration with ethanolamine oleate would be contraindicated because of the risk of tissue toxicity. Because 5% ethanolamine oleate is effective for management of varices [15], we used that concentration for cytolysis of the cyst epithelium. There is no consensus, however, on the appropriate volumes of ethanol and ethanolamine oleate for resolution of hepatic cysts. As suggested in a study of ethanol sclerosis [17], a volume of sclerosant equivalent to 10% of the volume of aspirated cystic fluid was injected in this study.

TABLE 1: Demographic and Cyst Characteristics of Patients with Symptomatic Hepatic Cysts

Patient No.	Age (y)	Sex	Symptoms	Diagnosis	Size (cm)	Estimated Cyst Volume (mL)	Volume Aspirated (mL)	Amount of Ethanolamine Oleate Injected (mL)	Follow-Up Period (mo)
1	67	M	Back pain	PLD	16×15	1,885	1,700	120	17
2	72	F	Epigastralgia	PLD	10.4×8.7	412	500	70	63
				Second episode	5.2×5.2	73	150	20	
3	86	F	Epigastralgia	PLD	7.7×6.8	185.7	150	16	1
4	72	F	Epigastralgia	PLD	9.1×8.3	328.2	400	40	2
5	45	F	Right hypochondrial pain	PLD	15×15	1,767.2	1,500	100	<1
6	63	M	Epigastralgia	PLD	14×11	887	1,550	100	<1
7	79	F	Abdominal distention	Simple cyst	4.3×3.4	26	34	10	84
8	70	F	Epigastralgia	PLD	7.4×7.2	200.9	120	15	9
9	75	M	Epigastralgia	PLD	8×7.1	211.6	400	60	56
				PLD	11.5×7.8	366.3	400	60	28
10	51	F	Abdominal distention	PLD	10.1×8.8	409.5	600	80	63
				PLD	6.5×6	122.5	350	40	62
11	60	F	Epigastralgia	PLD	11.9×10.8	726.8	1,620	120	54
				PLD	8.4×6.2	169.1	150	20	54
12	59	F	Epigastralgia	Simple cyst	9×9	381.7	350	40	72
13	54	F	Epigastralgia	PLD	15×15	1,767.2	1,000	100	95
				PLD	7×7	179.6	100	20	95

Note—PLD = polycystic liver disease.

After ethanolamine oleate injection, the pigtail catheter was clamped for 30 minutes. The patient was positioned supine for 10 minutes, on one side for 10 minutes, and on the other side for 10 minutes so that all of the cystic epithelium was exposed to the ethanolamine oleate. The ethanolamine oleate was aspirated from the cyst at the end of the procedure. The pigtail catheter was left in place for 24 hours of open drainage and was removed at the end of that period.

The effectiveness of ethanolamine oleate sclerosis of hepatic cysts was evaluated with follow-up ultrasound imaging or CT within 1 week of the procedure. Results of routine clinical blood tests (cell count, aspartate aminotransferase level, alanine aminotransferase level, bilirubin level) were followed for another week. In this series, follow-up ultrasound imaging or CT was performed 3, 6, 12, and 24 months after the procedure. The patients were monitored for adverse effects.

We calculated the data as mean, median, and SD and analyzed them with a spreadsheet program (Excel 2003, Microsoft). The Student's t test was used to test significance, which was set at $p < 0.05$.

Results

The patient and cyst characteristics are shown in Table 1. The symptoms included abdominal distention and abdominal pain. Nine patients had one cyst, and four patients had two cysts. The mean age of the patients was 65.6 ± 11.7 (SD) years (range, 45–72 years). Fifteen of the 17 cysts managed with percutaneous aspiration and ethanolamine oleate sclerosis were related to PLD; the other two were simple cysts. Both simple cysts were smaller than 10 cm in diameter. Eight PLD cysts had a maximum diameter greater than 10 cm, and seven measured less than 10 cm in diameter. The mean volume of the hepatic cysts was 589.8 ± 618.9 mL (range, 26–1,885 mL), and the mean amount of ethanolamine oleate needed for sclerosis was 57.3 ± 38.2 mL (range, 10–120 mL; median, 50 mL). The mean follow-up period was 44.4 ± 34.1 months (range, 1 week–95 months; median, 54 months).

The results of percutaneous aspiration and ethanolamine oleate sclerosis of symptomatic hepatic cysts and the complications are shown in Table 2. In all patients, pain and symptoms were relieved. The mean volumetric reduction of hepatic cysts with percutaneous aspiration and instillation of ethanolamine oleate was 88.8% ± 14.8% (range, 47.1–100%; median, 93.1%). The reduction was greatest for simple cysts (100% reduction) followed by PLD cysts larger than 10 cm (92.8% reduction) and PLD cysts smaller than 10 cm (80.7% reduction). The mean reduction 1 week, 3 months, and 1 year after treatment was 62.6%, 84.4%, and 96.4% respectively. All but one cyst resolved with a single session of ethanolamine oleate sclerosis; the one cyst required two sessions of instillations 3 months apart. There was no recurrence in any patient.

Table 3 compares the mean, median, and range of characteristics of the hepatic cysts. There are no significant differences in reduction between PLD cysts smaller than 10 cm and those larger than 10 cm. Nor were there

TABLE 2: Results and Complications of Percutaneous Hepatic Aspiration and Ethanolamine Oleate Sclerosis of Symptomatic Hepatic Cysts

Patient No.	Cyst Volume (mL)					Percentage Reduction			Complications
	Initial (n = 17)	1-wk Follow-Up (n = 16)	3-mo Follow-Up (n = 8)	1-y Follow-Up (n = 6)	Final (n = 17)	3-mo Follow-Up (n = 8)	1-y Follow-Up (n = 6)	Total (n = 17)	
1	1,885	294.5		157.3	157.4		91.7	91.7	Mild pain, no treatment required
2[a]	412	59.1	73.6	0.1	0	82.2	99.9	100	None
3	185.7	68.7			69.4			62.6	Mild pain, no treatment required
4[b]	328.2	N/A			173.9			47.0	Moderate abdominal and back pain, relieved with oral analgesic
5	1,767.2	238.9			238.9			86.5	Mild abdominal pain, right shoulder pain, no treatment required
6	887	139.1			139.1			84.4	None
7	26	26			0			100	Vasovagal reflex, improved with atropine; mild abdominal pain, no treatment required
8	200.9	70.8	31.5	0.7	0.7	84.3	99.7	99.7	Mild abdominal pain, no treatment required
9	211.6	171.9	43.6		29.4	79.4		86.1	None
	366.3	112.5		45.3	13.7		87.6	96.3	None
10	409.5	298.2	12.7		29.1	96.9		92.9	Mild right abdominal pain, no treatment required
	122.5	107.4	40.6		7.5	66.9		93.9	Right abdominal pain, distention; no treatment required
11	726.8	243.7	73.5		49.8	89.9		93.2	None
	169.1	60	32.3		41.6	80.9		75.4	None
12	381.7	50.3	19.6		0	94.9		100	Severe abdominal pain, relieved with oral analgesics
13	1,767.2	84.1		3.7	2.8		99.8	99.8	Mild abdominal pain, no treatment required
	179.6	14		0.3	0		99.8	100	Mild fever, no treatment required
Mean	589.8	122.6	44.4	34.6	56.2	84.4	96.4	88.4	

Note—N/A = not available.
[a]Patient 2 underwent two treatment sessions.
[b]Patient 4 underwent only a 1-month follow-up examination.

TABLE 3: Mean Reduction of Cyst Volume With Respect to Sex, Diagnosis, and Size of Cysts

Characteristic	No. of Cysts	Initial Cyst Volume (mL)			Mean Volume Reduction (%)	*p*
		Mean	Median	Range		
Patient sex						
Male	3	1,287.99 ± 933.9	1,767.2	1,885 – 211.6	87.3 ± 3.8	0.62
Female	14	440.2 ± 447.7	328.2	1,767.2 – 26	90.6 ± 16.1	
Nature of cystic disease						
Simple cyst	2	203.9 ± 251.5	203.9	381.7 – 26	100	0.99
Polycystic liver disease	15	641.3 ± 633.7	366.3	1,885 – 73.5	88.8 ± 15.2	
Size of cysts in polycystic liver disease						
> 10 cm	8	1,027.6 ± 669.5	806.9	1,885 – 366.3	94.5 ± 5.4	0.87
< 10 cm	7	199.7 ± 63.4	185.7	328.2 – 122.5	80.7 ± 20.1	

Note—NS = not significant.

differences between simple cysts and PLD in regard to efficacy of resolution with ethanolamine oleate therapy. Men and women also had similar results regarding resolution of cysts. Figure 1 shows the CT images of a liver cyst before and after sclerosis with ethanolamine oleate. That none of the patients needed surgical therapy for symptomatic PLD in the follow-up period resulted in excellent quality of life.

No major complications occurred that could have been considered life-threatening or precluding treatment. There was, however, one episode of vasovagal attack, which was managed with conservative treatment without stopping the ethanolamine oleate sclerosis treatment session. In six of the 17 cases of cyst treatment (35.3%), the patient had no pain or complications. In nine cases (52.9%), the patient had mild pain, which did not require analgesics and two patients had moderate to severe abdominal pain necessitating oral analgesics, and one patient (11.1%) had a self-resolving mild fever.

Discussion

Minimally invasive techniques such as ethanol sclerosis have been disappointing in the management of PLD in spite of relative success in resolution of simple hepatic cysts. Previous reports [1, 7] have suggested high recurrence rates among patients with PLD, some reports showing a greater than 75% recurrence rate. Furthermore, resolution with ethanol as a sclerosing agent occurs in fewer than 25% of patients with PLD. The results are better for simple cysts, in the range of 80–90% [3–7]. The poorer long-term treatment response among PLD patients may be due to the more rigid hepatic architecture in polycystic than in normal livers, which results in inadequate cyst collapse [19–23] during the aspiration phase of treatment. In our study, percutaneous aspiration and ethanolamine oleate sclerosis led to resolution of 15 of 15 PLD cysts in only one treatment session in 93.3% (14/15) of cases and two sessions in 6.7% (1/15) of cases.

Our results are groundbreaking compared with the previous techniques of simple percutaneous aspiration with or without ethanol sclerosis and surgical therapy. Percutaneous aspiration alone has an almost 100% recurrence rate [4], and its role is limited only to a diagnostic tool for establishing the link between the hepatic cyst and the symptoms [1]. Percutaneous aspiration of a cyst followed by instillation of ethanol has not resulted in sustained reduction in cyst volume. Erdogan et al. [1] found a recurrence rate of 78.7% within a few months of ethanol sclerosis of PLD, and a second attempt at sclerosis did not improve the efficacy of cyst resolution. Other studies [7, 20] have shown similarly high recurrence rates and poor cyst and symptom resolution. We believe the success of percutaneous aspiration with ethanolamine oleate sclerosis for cyst resolution in our study may have been primarily due to the use of ethanolamine oleate and the technique used. Improved resolution with ethanolamine oleate probably occurred because ethanolamine oleate is more effective than alcohol in destroying the epithelium of the cyst. Exposure to ethanolamine oleate leads to cytolysis followed by thrombogenesis. The ethanolamine oleate functions as a cytolytic agent owing to its anionic surfactant properties that brings about a change in cellular permeability [17].

We used an innovative method of leaving the ethanolamine oleate catheter in place with open drainage for 24 hours. Aspiration of the cystic contents led to collapse of the cyst, resulting in better exposure of the endothelium of the cyst wall to the ethanolamine oleate. We believe the walls of PLD cysts are stiffer and less likely to collapse than those of other cysts and are therefore responsible for the high recurrence rate. It is probable that this technique of open drainage for 24 hours may have caused the cyst to remain collapsed, ensuring greater contact between the cyst epithelium and the ethanolamine oleate and enabling more efficient and sustained sclerosis. None of the patients needed surgical therapy for symptomatic PLD in the follow-up period. All patients in this study experienced relief of the pretreatment symptoms and had excellent quality of life after treatment.

Except for mild to moderate pain in approximately 60% of patients, there were no major adverse effects. The other 40% of patients had no adverse effects. No late-onset adverse reactions were apparent in the long-term follow-up period of up to 95 months. In contrast, several cases of complications have been associated with ethanol sclerosis [7, 11], the incidence being approximately 6.7% [1]. Complications of the use of percutaneous ethanol for ablation therapy can occur during placement of the needle into the target organ or tissue or as a result of injection of ethanol into the body. Complications related to injection of ethanol may be secondary to absorption of ethanol into the bloodstream or to unintentional intravascular injection. Absorbed ethanol can cause various degrees of intoxication and hypotension. In addition, one of the metabolites of ethanol, acetaldehyde acetate, can cause hypotension by inducing peripheral vasodilatation. Normally, the enzyme acetaldehyde dehydrogenase neutralizes acetaldehyde ac-